Magnetic Reconnection in the Lower Solar Atmosphere

Vyacheslav (Slava) Lukin

National Science Foundation*

Collaborators: Nick Murphy (CfA), Eric Meier (William & Mary), Elena Provornikova (UCAR/NRL),

Martin Laming, James Leake, Mark Linton (NRL)

University of Michigan – Ann Arbor September 19th, 2016



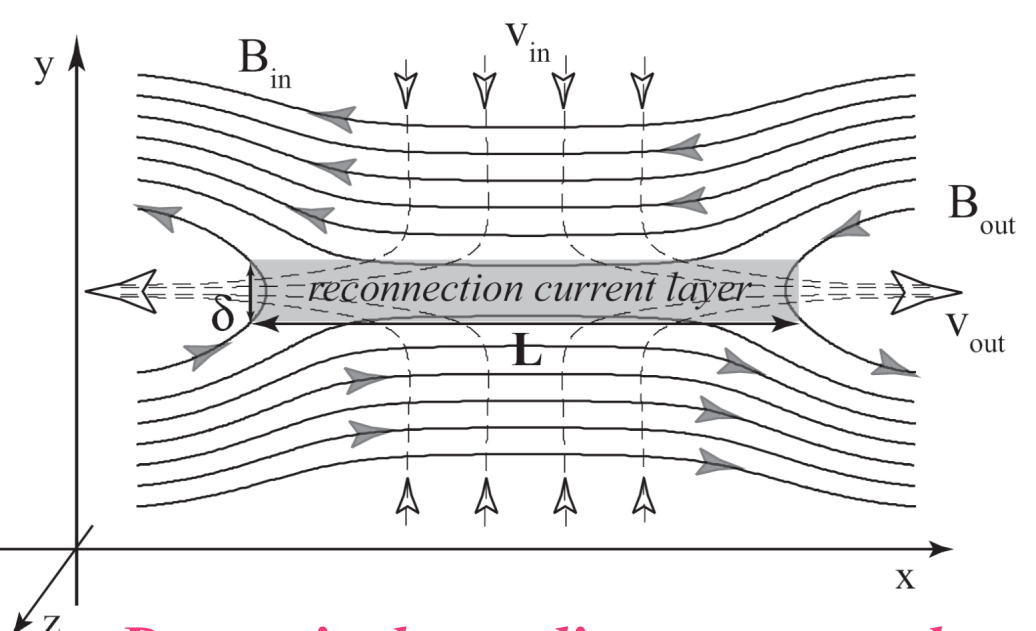
* Any opinion, findings, and conclusions or recommendations expressed in this material are those of the authors and do not necessarily reflect the views of the National Science Foundation.

Outline

- ➤ Motivation: Magnetic Reconnection everywhere... and in the Lower Solar Atmosphere
- ➤ HiFi modeling framework and the partially ionized reacting multifluid model
- Magnetic reconnection in a weakly ionized plasma
 - ☐ Structure and scalings of a laminar reconnection region
 - Onset of the plasmoid instability
 - ☐ Asymmetric reconnection
 - ☐ Ion inertial effects the Hall effect
- ➤ Plasma compressibility in coronal reconnection sites implications for particle acceleration



Magnetic Reconnection



Local reconfiguration and annihilation of magnetic fields resulting in relaxation of the global topology of a magnetic configuration in such a way as to transfer energy stored in the stressed magnetic fields into kinetic (directed) and thermal (random) energy of the plasma.

Dynamical coupling across orders of magnitude in spatial scales!

Where does/could magnetic reconnection play a role?

Astrophysics:

- pulsar magnetospheres
- heating of interstellar and intergalactic medium
- dynamics of accreting systems

Space & Solar Physics:

- solar flares, coronal mass ejections
- solar corona heating
- interaction of solar wind with planetary magnetospheres

Magnetic Fusion Devices:

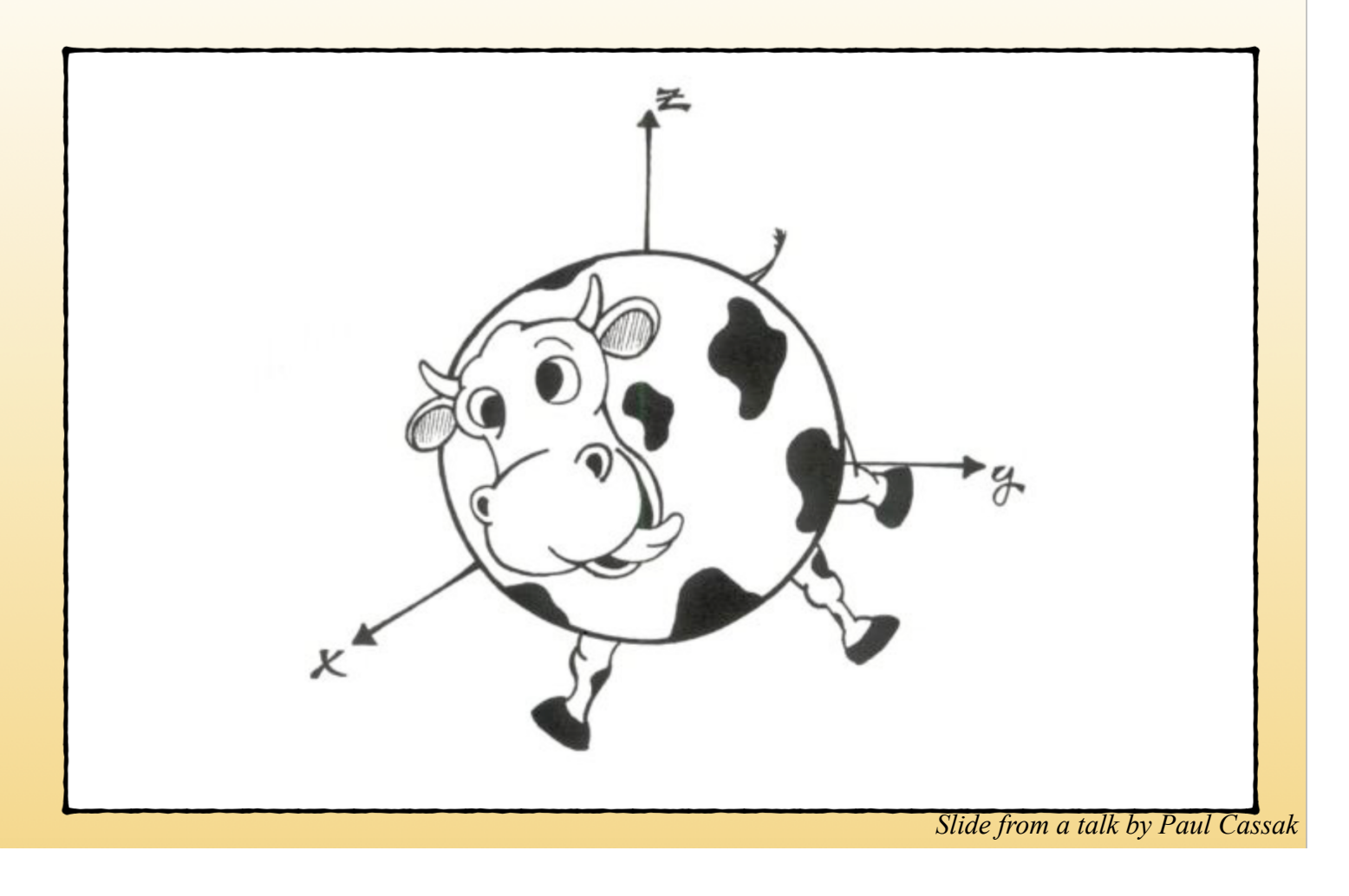
- sawtooth crash and tearing instability in toroidal devices
- coaxial helicity injection
- self-reversal in

Reversed-Field Pinch devices



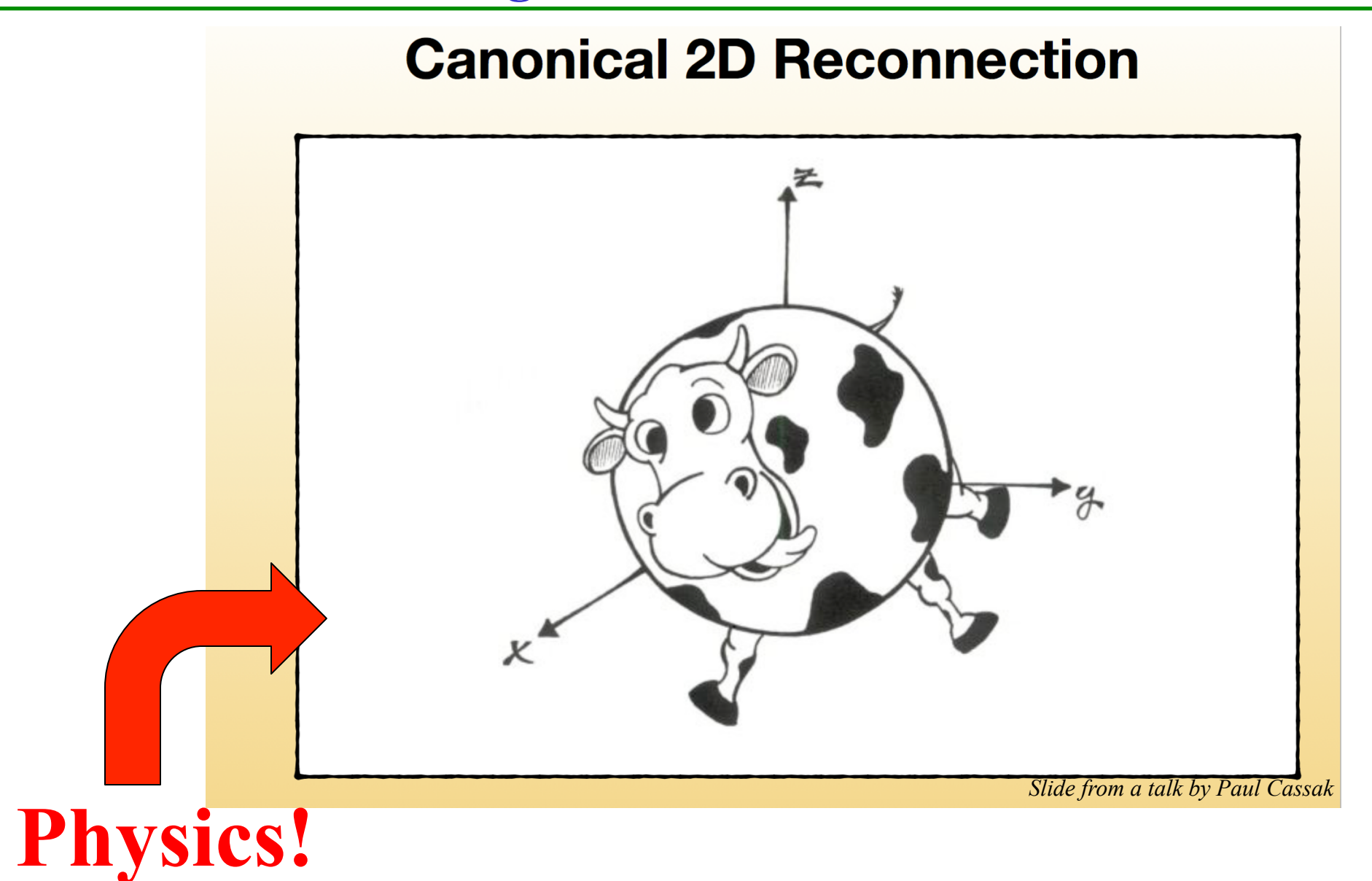
Magnetic Reconnection

Canonical 2D Reconnection





Magnetic Reconnection





How Does Magnetic Reconnection Happen?

Generic High Level Timeline:

- 1. Free magnetic energy is supplied into some <u>large-scale volume</u>.
 - a. pre-existing magnetic structures are convected towards each other; e.g., two flux ropes are convected into each other;
 - b. magnetic fields are stressed in-place; this could be fast or slow (relative to the Alfven time), could be quasi-random on small scales or organized on large scales; e.g., magnetic loops tangled by field line footpoint motions in the solar photosphere;
- 2. Magnetic field lines begin to reconnect with each other over some <u>set of small-scale sub-volumes</u>;
- 3. Free magnetic energy is released in the form of flows, heat, radiation and non-thermal particle acceleration;

Energy may be released locally within the reconnection sub-volumes [e.g., Joule heating, radiation, and particle acceleration], or globally due to the reconfiguration of the fields that has been allowed by reconnection.



Key Questions in Magnetic Reconnection

➤ How fast can the magnetic energy be released?

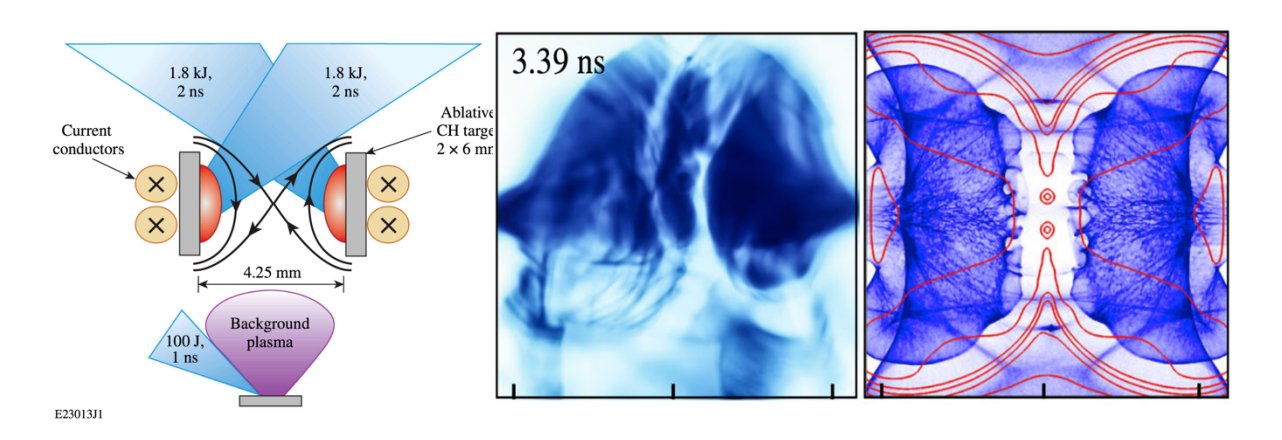
➤ How is it possible that under some circumstances free magnetic energy can be slowly accumulated and then explosively released?

➤ What determines the released energy partition between thermal, radiation, bulk flow and non-thermal particles?

➤ Under what circumstances the reconnection sub-volumes are localized in 1D (a current sheet), 2D (a line current) and 3D (a point-like current density concentration)?

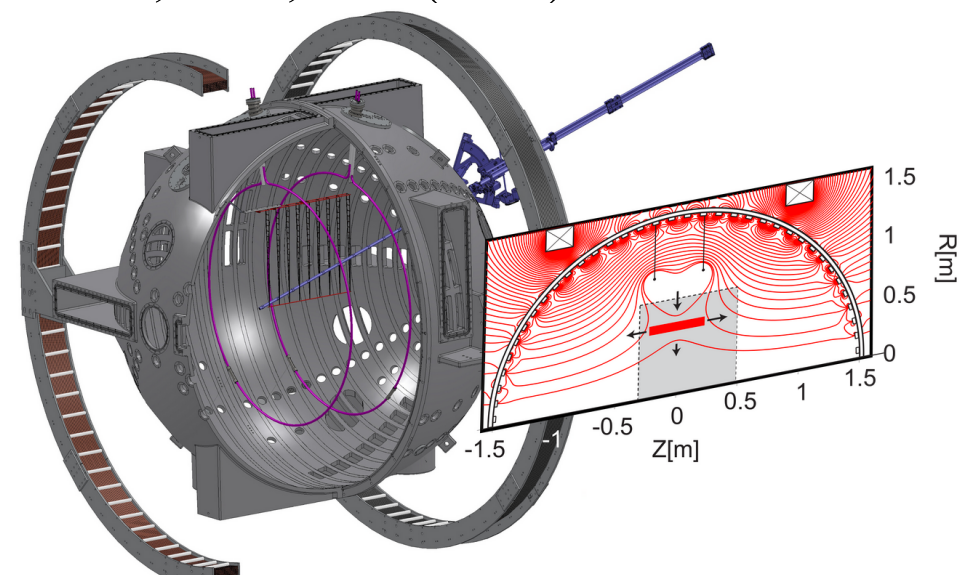


Magnetic Reconnection – Dedicated Experiments

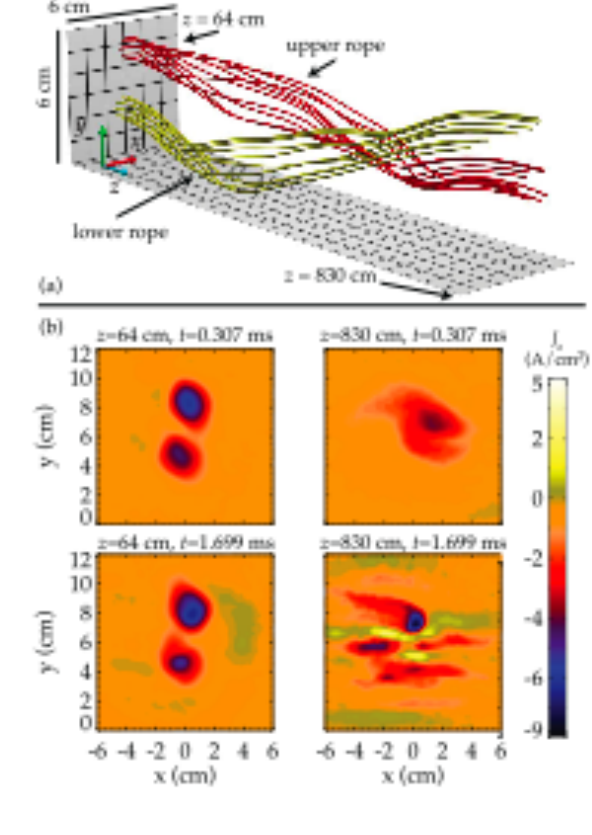


Reconnection between Laser-Produced Plasma Plumes Fiksel, et al., PRL (2014)

Terrestial
Reconnection
eXperiment
(TREX)
Olson, Egedal
et al., PRL
(2016)

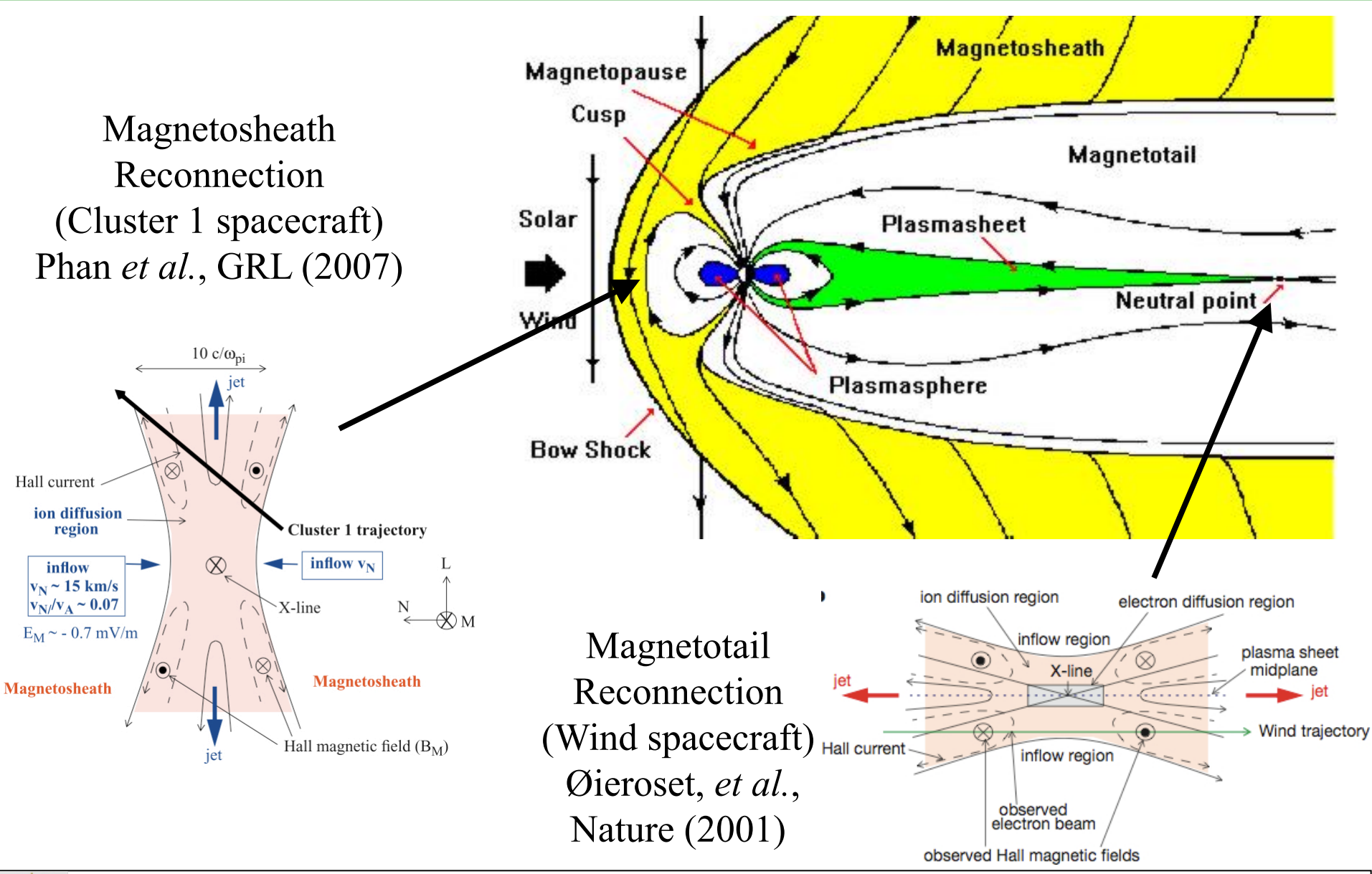


LArge Plasma Device Lawrence & Gekelman PRL (2009)



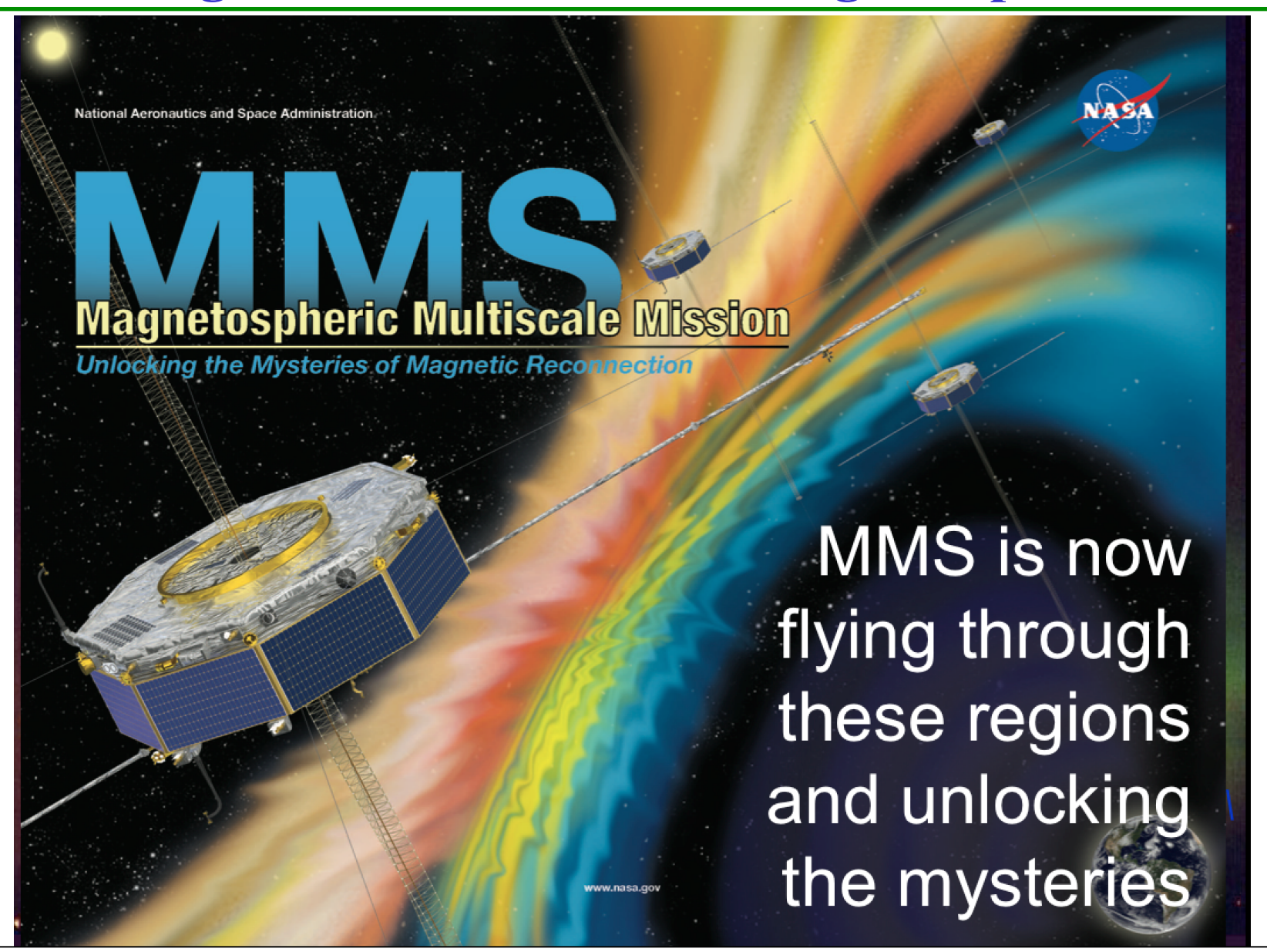


Magnetic Reconnection – Magnetosphere



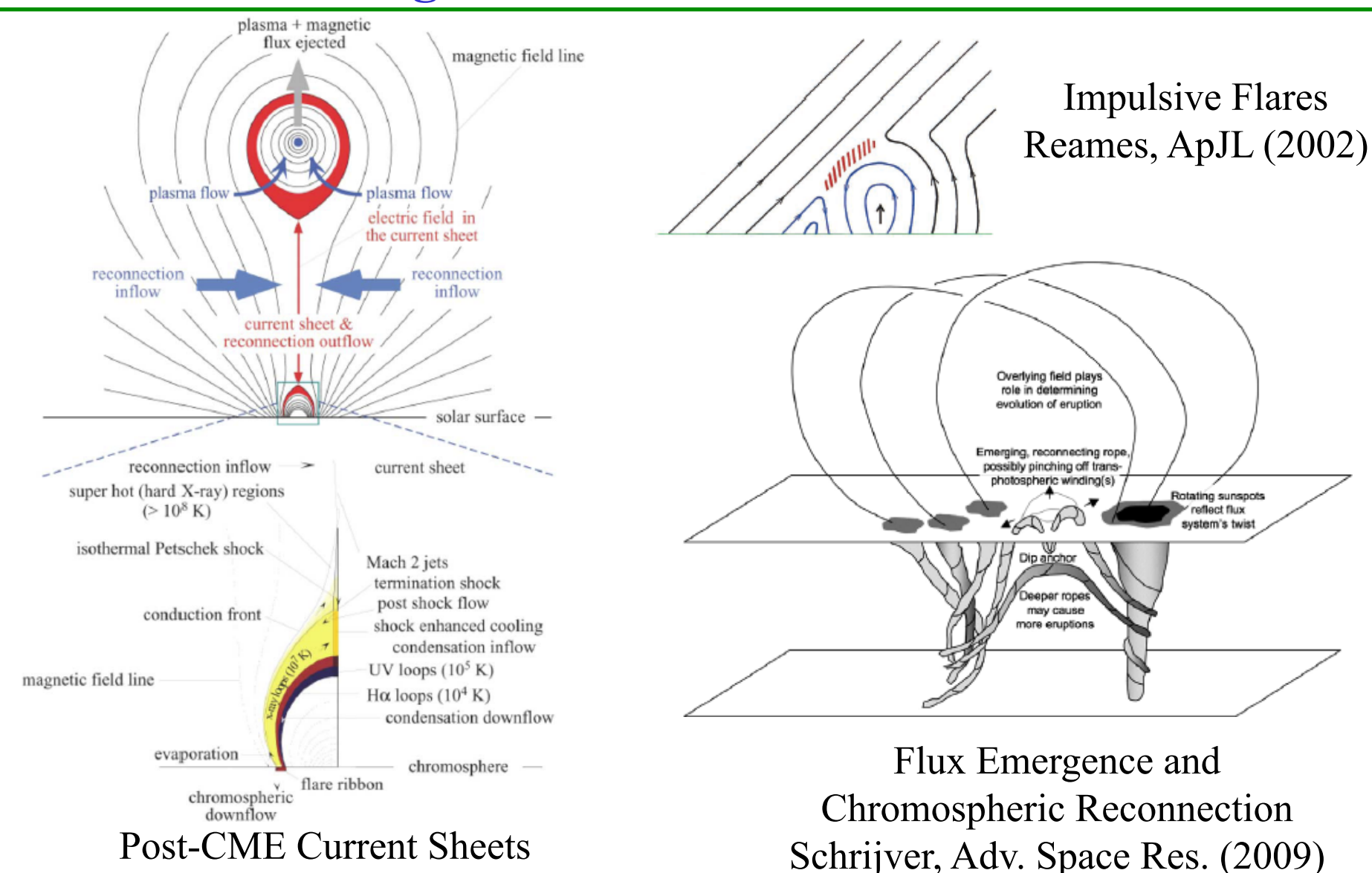


Magnetic Reconnection – Magnetosphere





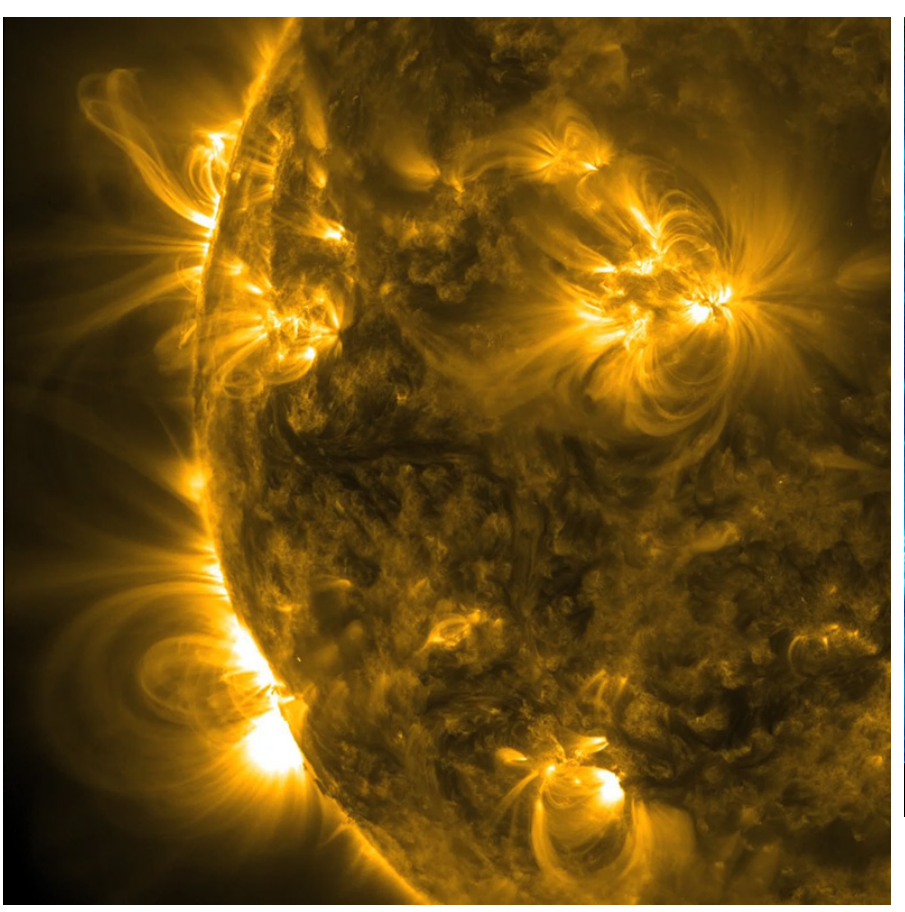
Magnetic Reconnection – Solar

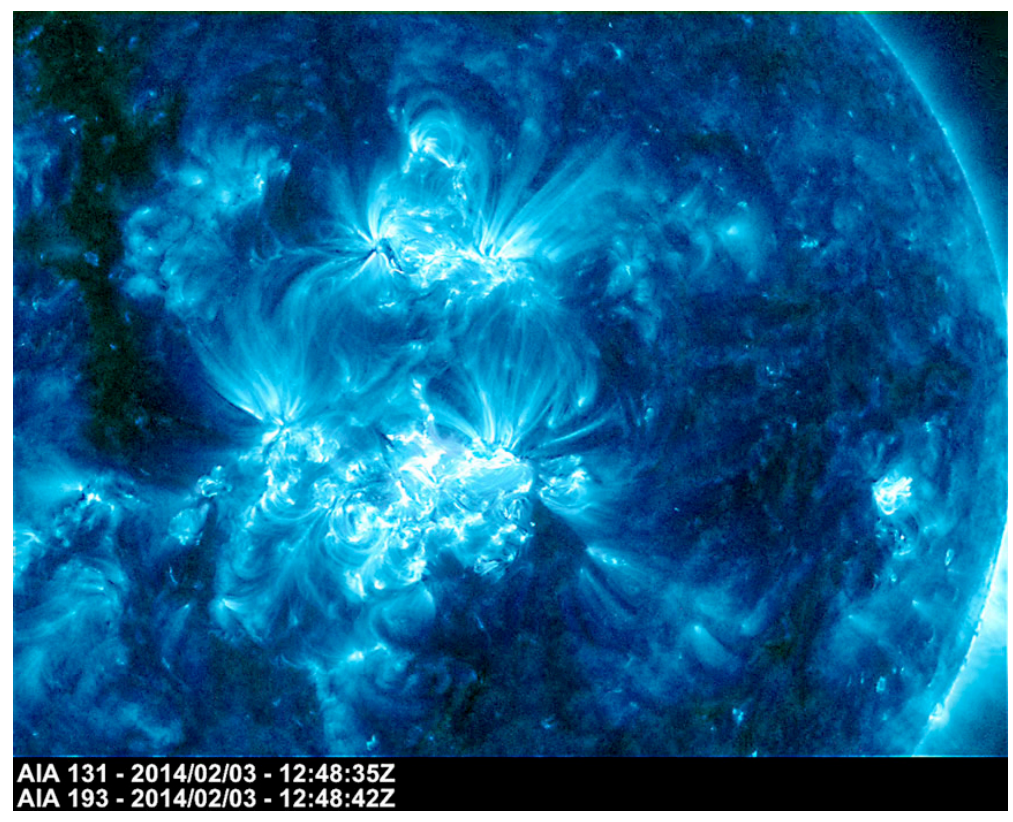




Lin *et al.*, JGR (2008)

Magnetic Reconnection – Solar Corona





Images courtesy of NASA / Solar Dynamics Observatory

Magnetic activity in the solar corona, from active regions to formation of the fast and slow solar wind, is mediated by magnetic reconnection



Magnetic Reconnection – Solar Chromosphere

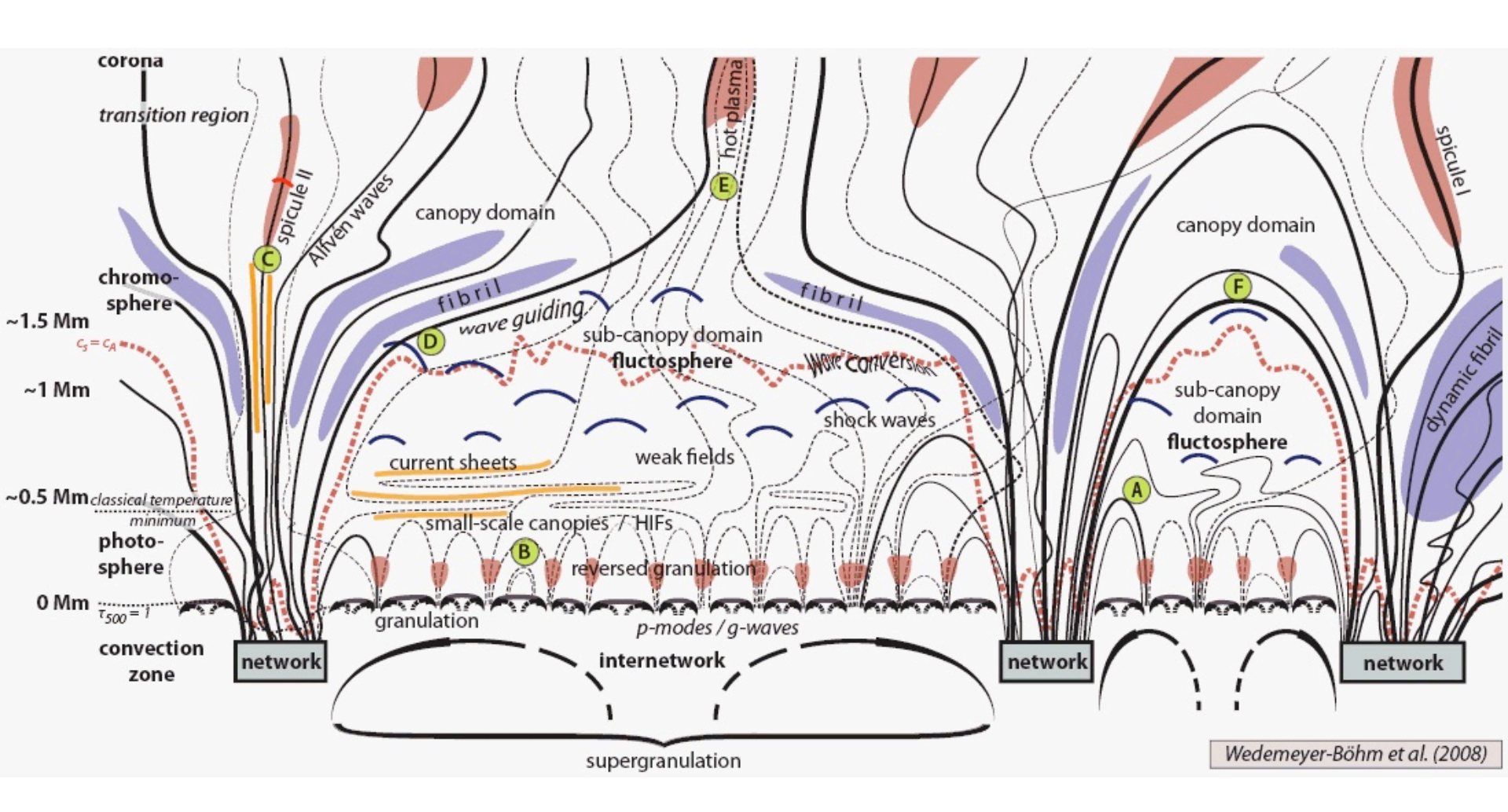
And below that...



Image courtesy of Bart De Pontieu; NASA / Interface Region Imaging Spectrograph



Solar Chromosphere





What is Unique About the Chromosphere?

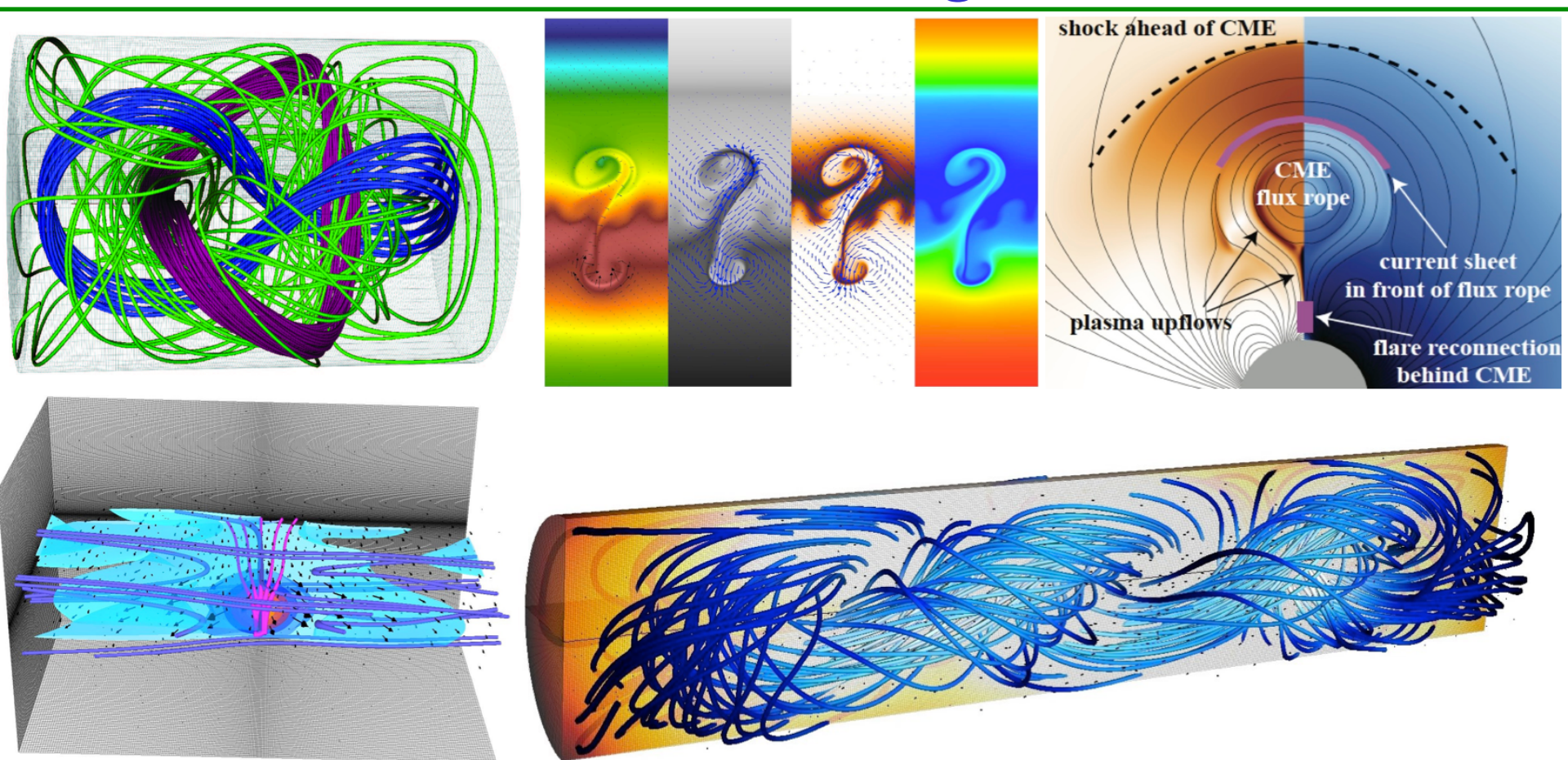
- 1. A relatively thin, \sim 2 Mm, boundary layer between the pressure / flow / radiation dominated convection zone and the magnetically dominated corona
 - ✓ Average particle density changes by several orders of magnitude from the bottom to the top of the chromosphere
 - ✓ Plasma beta changes from >> 1 at the bottom to < 1 at the top of the chromosphere
- 2. Due to the density and temperature variations with height, plasma ionization fraction varies from $\sim 0.1\%$ to $\sim 50\%$
 - ✓ Non-equilibrium ionization-recombination effects can be dynamically important
 - ✓ While the plasma is hydrogen dominated, there are regions where the ionized fraction is dominated by heavy low first ionization potential (FIP) elements
- 3. Radiation transport is highly complex, changing with height from optically thick to optically thin
 - ✓ Radiation transport effects can also impact ionization and recombination rates
- 4. The above statements about height dependence are nominal... There are O(1) horizontal variations in magnetic field strength, particle density, temperature, etc.



HiFi Multi-Fluid Modeling Framework



HiFi Multi-Fluid Modeling Framework



Sample images from simulations of magnetized plasmas in laboratory and space performed within the <u>HiFi multi-fluid modeling framework</u> and visualized with the <u>VisIt visualization tool</u>.

Open-source 2D & 3D modeling framework with operational versions of the code freely available under a BSD-style license. For more info, see: http://hifi-framework.webnode.com/hifi-framework/



HiFi Multi-Fluid Modeling Framework

- ➤ Open source platform to model behavior of fluid-based dynamical systems as initial value solutions of non-linear coupled PDEs
- ➤ High-order local spatial discretization and implicit time advance
- > General standard "flux-source" format for equations to be solved
- Main algorithm compiled into a library that is transparently used by the user-specified *physics* file constructed according to a provided generic template
- > Template designed for a computationally-oriented graduate student
- ➤ Allows user (application scientist) to specify:
 - Application-specific input deck, initial conditions and spatial grid
 - Desired PDEs in the coordinate system of one's choosing
 - Desired boundary conditions



Reacting Multi-Fluid Model in HiFi

Continuity:

Due to charge neutrality, only the ion and neutral continuity equations are required.

$$rac{\partial n_i}{\partial t} +
abla \cdot (n_i \mathbf{v}_i) = \Gamma_i^{ion} + \Gamma_i^{rec}, \qquad ionization \ \frac{\partial n_n}{\partial t} +
abla \cdot (n_n \mathbf{v}_n) = \Gamma_n^{rec} + \Gamma_n^{ion}. \qquad recombination \ .$$

Momentum:

The electron and ion momentum equations are summed and terms of order $(m_e/m_p)^{1/2}$ and higher are neglected to give:

$$\frac{\partial}{\partial t}(m_i n_i \mathbf{v}_i) + \nabla \cdot (m_i n_i \mathbf{v}_i \mathbf{v}_i + \mathbb{P}_i + \mathbb{P}_e) = \mathbf{j} \times \mathbf{B} + \mathbf{R}_i^{in} + \Gamma_i^{ion} m_i \mathbf{v}_n - \Gamma_n^{rec} m_i \mathbf{v}_i + \Gamma^{cx} m_i (\mathbf{v}_n - \mathbf{v}_i) + \mathbf{R}_{in}^{cx} - \mathbf{R}_{ni}^{cx}.$$

$$charge-exchange$$

The neutral momentum equation is

$$\frac{\partial}{\partial t}(m_i n_n \mathbf{v}_n) + \nabla \cdot (m_i n_n \mathbf{v}_n \mathbf{v}_n + \mathbb{P}_n) = -\mathbf{R}_i^{in} + \Gamma_n^{rec} m_i \mathbf{v}_i - \Gamma_i^{ion} m_i \mathbf{v}_n + \Gamma_n^{cx} m_i (\mathbf{v}_i - \mathbf{v}_n) - \mathbf{R}_{in}^{cx} + \mathbf{R}_{ni}^{cx}.$$



Reacting Multi-Fluid Model in HiFi

Internal Energy:

Again, combining the electron and ion energy equations together and neglecting terms of the order $(m_e/m_p)^{1/2}$ and higher gives:

$$\begin{split} \frac{\partial}{\partial t} \left(\boldsymbol{\varepsilon}_{i} + \frac{P_{e}}{\gamma - 1} \right) &+ \nabla \cdot \left(\boldsymbol{\varepsilon}_{i} \mathbf{v}_{i} + \frac{P_{e} \mathbf{v}_{e}}{\gamma - 1} + \mathbf{v}_{i} \cdot \mathbb{P}_{i} + \mathbf{v}_{e} \cdot \mathbb{P}_{e} + \mathbf{h}_{i} + \mathbf{h}_{e} \right) = \mathbf{j} \cdot \mathbf{E} \\ &+ \mathbf{v}_{i} \cdot \mathbf{R}_{i}^{in} + Q_{i}^{in} - \Gamma_{n}^{rec} \frac{1}{2} m_{i} v_{i}^{2} - Q_{n}^{rec} + \Gamma_{i}^{ion} (\frac{1}{2} m_{i} v_{n}^{2} - \phi_{eff}) + Q_{i}^{ion} \\ &+ \Gamma^{cx} \frac{1}{2} m_{i} \left(\mathbf{v}_{n}^{2} - \mathbf{v}_{i}^{2} \right) + \mathbf{v}_{n} \cdot \mathbf{R}_{in}^{cx} - \mathbf{v}_{i} \cdot \mathbf{R}_{ni}^{cx} + Q_{in}^{cx} - Q_{ni}^{cx}. \end{split}$$

The neutral energy equation is

optically thin radiative losses

$$\begin{split} \frac{\partial \varepsilon_n}{\partial t} &+ \nabla \cdot (\varepsilon_n \mathbf{v}_n + \mathbf{v}_n \cdot \mathbb{P}_n + \mathbf{h}_n) \\ &= &- \mathbf{v}_n \cdot \mathbf{R}_i^{in} + Q_n^{ni} - \Gamma_i^{ion} \frac{1}{2} m_i \mathbf{v}_n^2 - Q_i^{ion} + \Gamma_n^{rec} \frac{1}{2} m_i \mathbf{v}_i^2 + Q_n^{rec} \\ &+ &\Gamma^{cx} \frac{1}{2} m_i (\mathbf{v}_i^2 - \mathbf{v}_n^2) + \mathbf{v}_i \cdot \mathbf{R}_{ni}^{cx} - \mathbf{v}_n \cdot \mathbf{R}_{in}^{cx} + Q_{ni}^{cx} - Q_{in}^{cx}. \end{split}$$



Reacting Multi-Fluid Model in HiFi

Ohm's Law:

We drop the electron inertia and the viscous part of the electron pressure tensor but include electron-neutral collisions as well as electron-ion collisions:

$$\mathbf{E} + (\mathbf{v}_i \times \mathbf{B}) = \eta \mathbf{j} + \frac{\mathbf{j} \times \mathbf{B}}{en_i} - \frac{1}{en_i} \nabla P_e - \frac{m_e \nu_{en}}{e} \mathbf{w}, \quad \begin{array}{c} \text{``three-fluid'' terms} \\ \text{accounting for} \\ \text{separate electron flow} \end{array}$$

where $\mathbf{w} = \mathbf{v}_i - \mathbf{v}_n$. The resistivity η is calculated using the electron-ion and electron-neutral collisional frequencies, and thus depends on the plasma conditions:

$$\eta = \frac{m_e n_e (\nu_{ei} + \nu_{en})}{(en_e)^2}$$

where the electron-ion (ν_{ei}) and electron-neutral (ν_{en}) collision frequencies are given by

$$u_{ei} = \frac{4}{3} n_i \Sigma_{ei} \sqrt{\frac{2k_B T_e}{\pi m_e}}, \text{ and } \nu_{en} = n_n \Sigma_{en} \sqrt{\frac{8k_B T_{en}}{\pi m_{en}}}.$$



Magnetic Reconnection in a Weakly Ionized Plasma of Solar Chromosphere



Key Questions in Magnetic Reconnection

- ➤ How fast can the magnetic energy be released?
 - **Could the partial ionization effects impact / accelerate the reconnection rate?**
- ➤ How is it possible that under some circumstances free magnetic energy can be slowly accumulated and then explosively released?
 - **Could the partial ionization effects enable a transition from slow to fast reconnection in the chromosphere?**
- ➤ What determines the released energy partition between thermal, radiation, bulk flow and non-thermal particles?
 - ❖ How do the partial ionization effects impact the energy partitioning at different heights within the chromosphere?
- ➤ Under what circumstances the reconnection sub-volumes are localized in 1D (a current sheet), 2D (a line current) and 3D (a point-like current density concentration)?
 - * Could the partial ionization effects impact the physics of reconnection region localization?



Magnetic Reconnection – Laminar Resistive Theory

 $\boldsymbol{B}_{\text{in}}$

Parker (1957), Sweet (1958)

In the standard 2D cartoon, the local magnetic field annihilation takes place within an elongated current diffusion region:

$$\omega \equiv (\delta/L) \ll 1$$

 $=> \left\{ \begin{array}{ccc} E_R = V_{in}B_{in} & = & V_{out}B_{out} = D(\eta,J_0) \\ \hline V_{in}L & = & V_{out}\delta \\ \hline V_{out} & = & B_{in} \end{array} \right.$

Derived from the continuity equation. Assumes no sources / sinks of particles in the diffusion region

reconnection current tayer=

 $\mathbf{B}_{\mathrm{out}}$

Vout

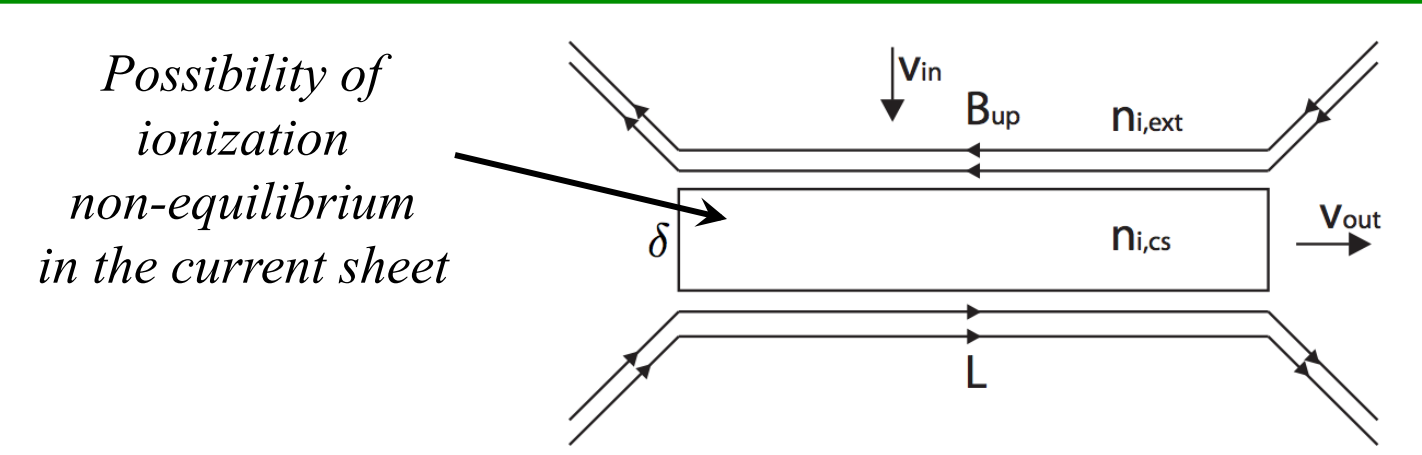
where $D(\eta, J)$ is the magnetic diffusion operator.

If magnetic field diffusion is resistive:

$$rac{v_{
m in}}{v_A}pprox \sqrt{rac{\eta}{v_A L \mu_0}}=\sqrt{rac{\eta}{v_A L \mu_0}}$$



Magnetic Reconnection – Weakly Ionized Regime



Continuity Eq.:
$$n_{i,\text{ext}}v_{\text{in}}L = n_{i,\text{CS}}(\delta v_{\text{out}} + \delta L v^{\text{rec}} - \delta L v^{\text{ion}})$$

It follows that:
$$v_{\rm in} \approx \sqrt{\frac{\eta}{\mu_0} \frac{n_{i,\rm CS}}{n_{i,\rm ext}}} (v_{\rm out} + v^{\rm rec} - v^{\rm ion})$$
, where $v_{\rm out} \equiv v_{\rm out}/L$

If the system is in <u>ionization – recombination balance</u>, the reconnection rate can be enhanced due to the ambipolar diffusion effects, but the <u>single-fluid resistive</u> <u>scaling</u> does not fundamentally change.

If <u>recombination dominates</u>, the Sweet-Parker outflow bottleneck can be avoided and the system allows for <u>'fast' resistivity-independent reconnection rate</u>.

Vishniac & Lazarian, ApJ (1999); Heitsch & Zweibel, ApJ (2003)



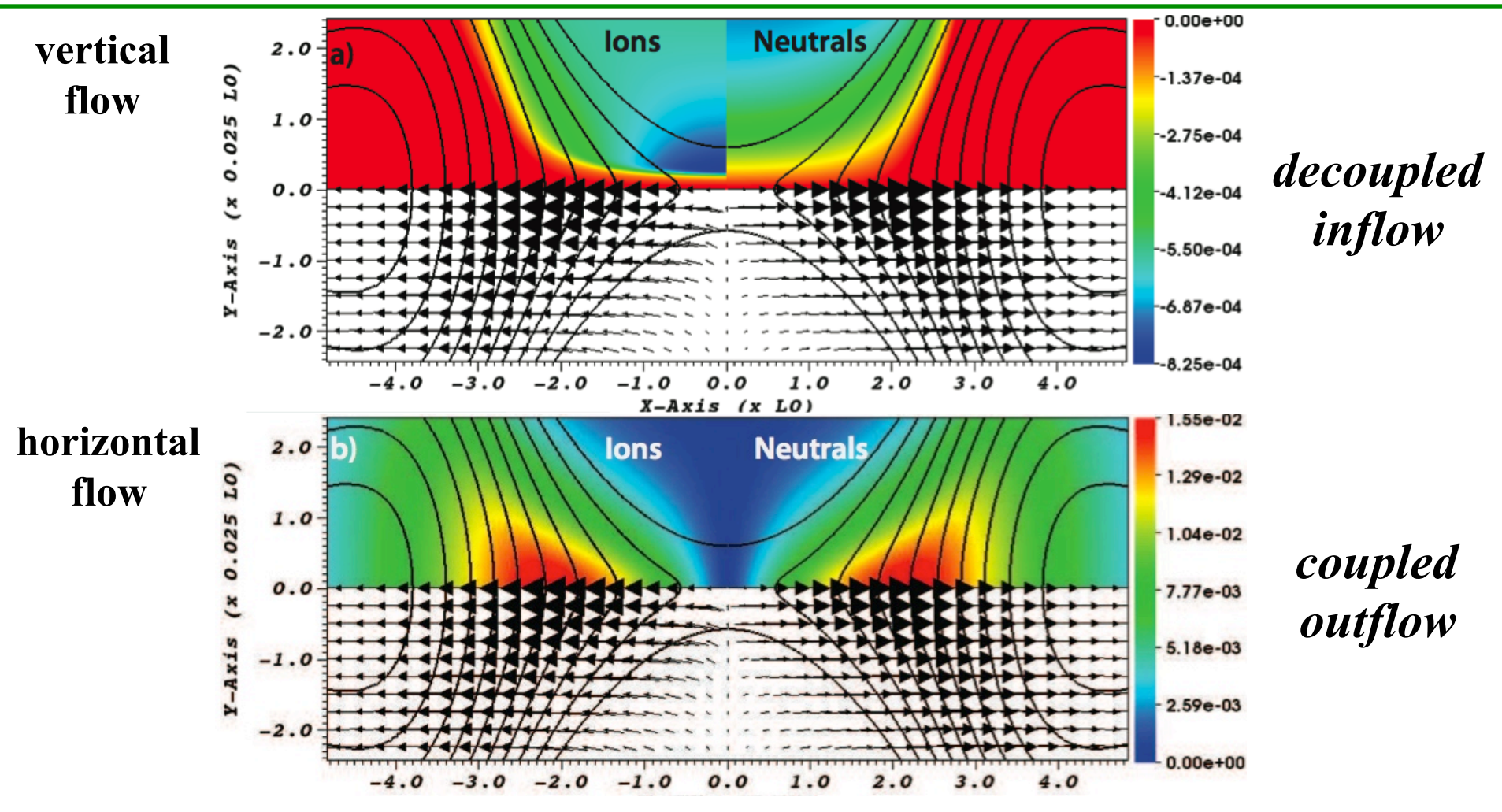
Weakly Ionized Regime – 2D HiFi Simulations

plasma
parameters
characteristic
of lower
to middle
chromosphere

- Length scale (L0) $\sim 10 100 \text{ km}$
- Neutral-ion collisional mean free path, $\lambda_{ni} \sim 0.1 1 \text{ km}$
- Reconnecting magnetic field strength (B0) ~ 10 Gauss
- Background electron & ion number density $\sim 10^9 10^{10}$ cm⁻³
- Neutral hydrogen atom number density $\sim 10^{12} 10^{13}$ cm⁻³
- Background ionization fraction ~ 0.1%
- Plasma temperature ~ 8500 K
- Alfven speed based on ion mass density ~ 100 km/s
- Alfven speed based on total mass density ~ 3.5 km/s

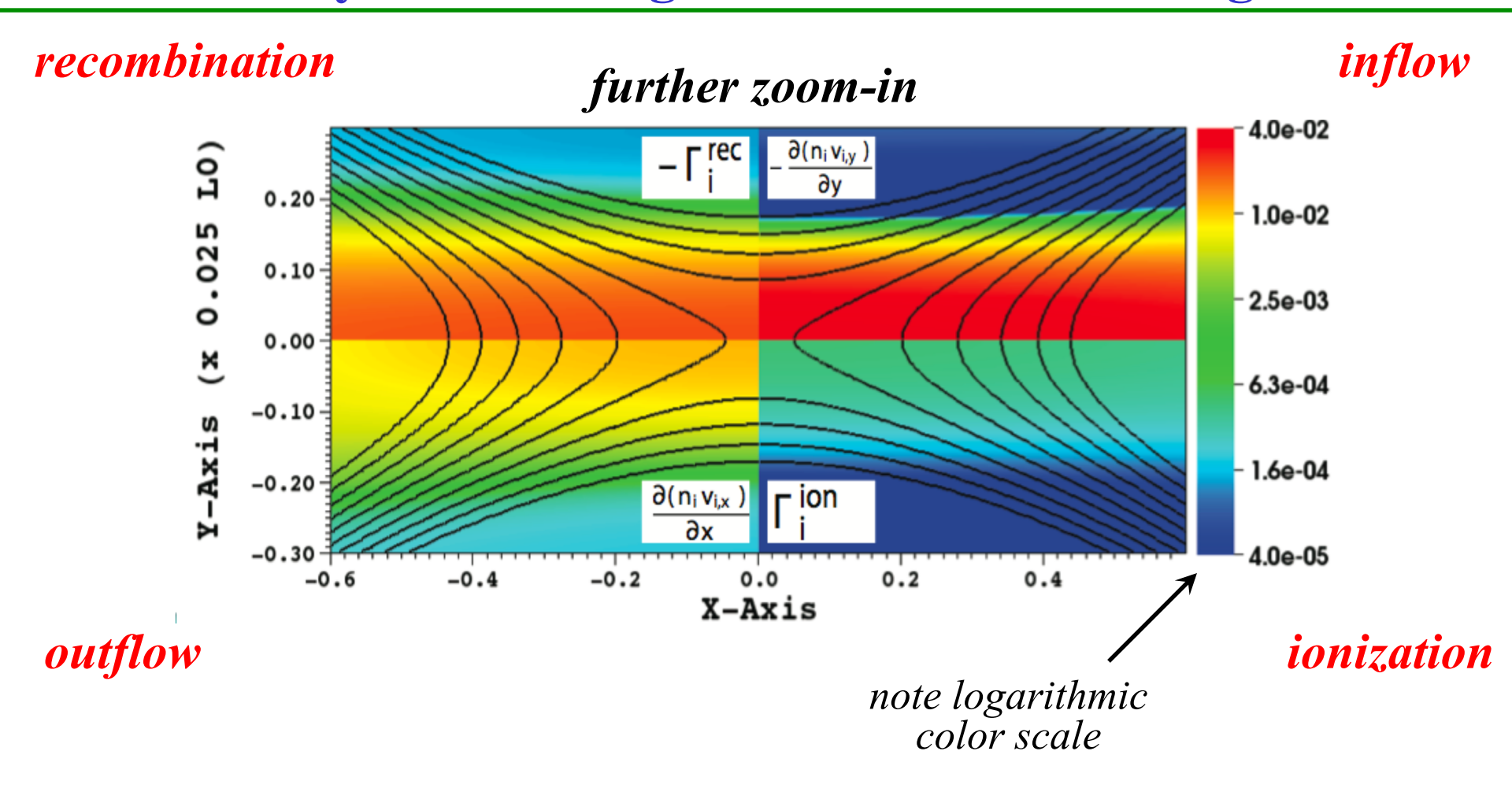
Leake, Lukin, Linton & Meier, ApJ (2012); Leake, Lukin & Linton, PoP (2013)





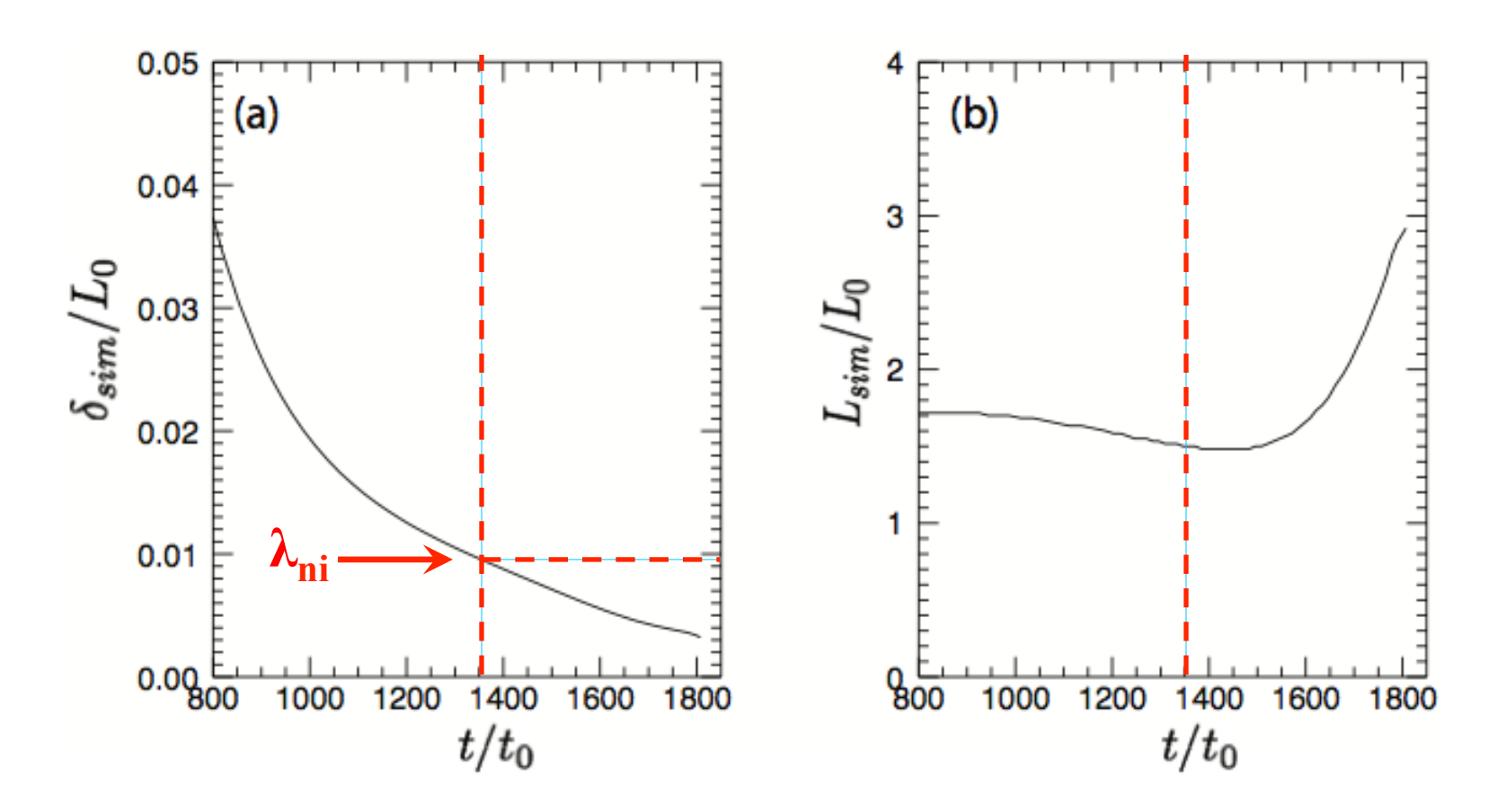
Inflows decouple when the resistive current sheet diffusion scale becomes smaller than the neutral-ion collisional mean free path, $\lambda_{ni} \sim 100$ m.





Recombination and, to a lesser degree, ion (electron) outflow balance the ion (electron) inflow into the reconnection region.

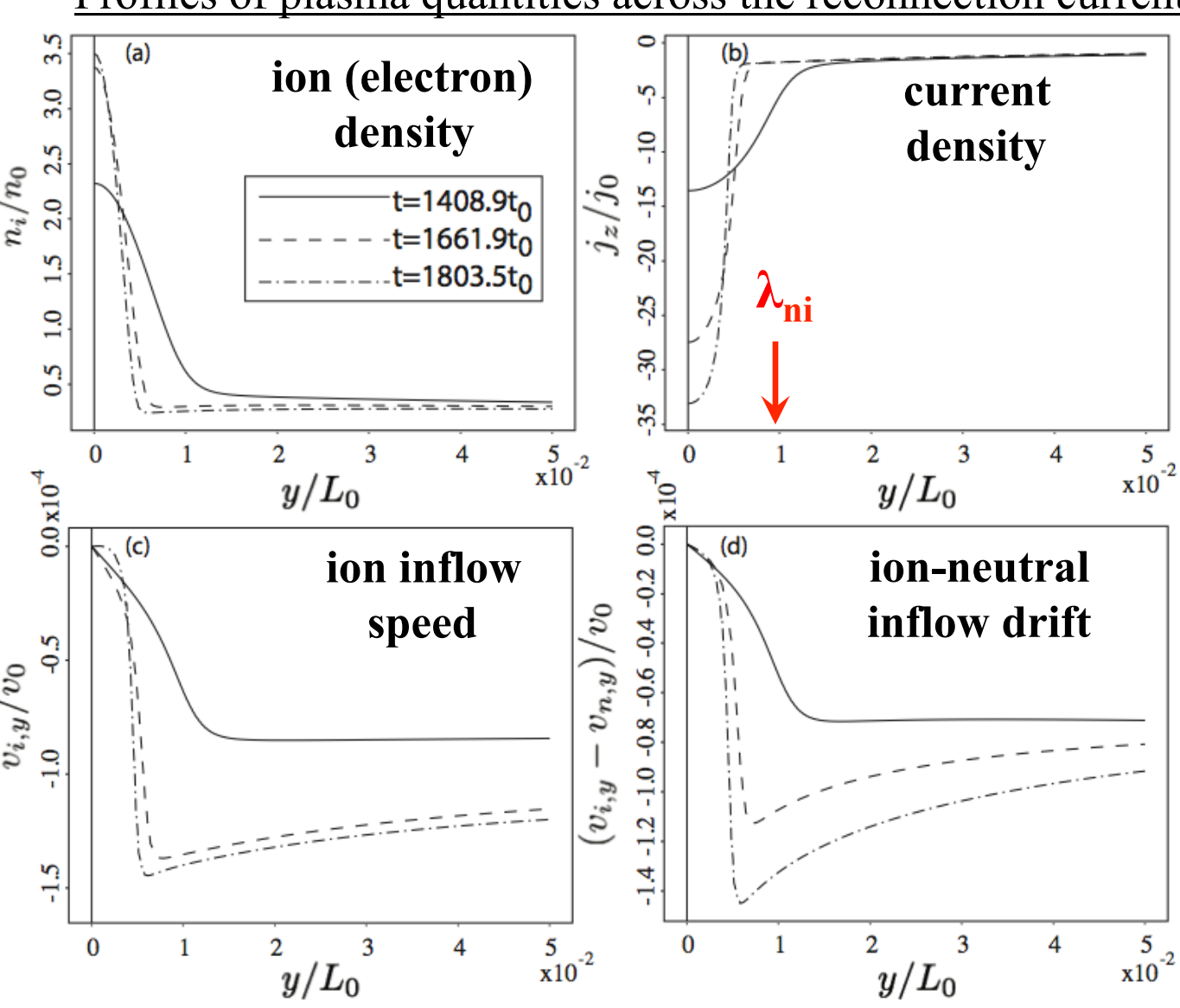




As the fully nonlinear reconnection region forms out of the initial small and localized perturbation, the thickness of the current layer continues to decrease, while its length begins to increase.



Profiles of plasma quantities across the reconnection current sheet



- 1) ion density in the current sheet is greater than the background value by an order of magnitude
- 2) ion inflow velocity increases just upstream of the current sheet ions are sucked into the current sheet
- 3) ion inflow is much faster than neutral inflow



Weakly Ionized Regime: Aspect Ratio Scaling

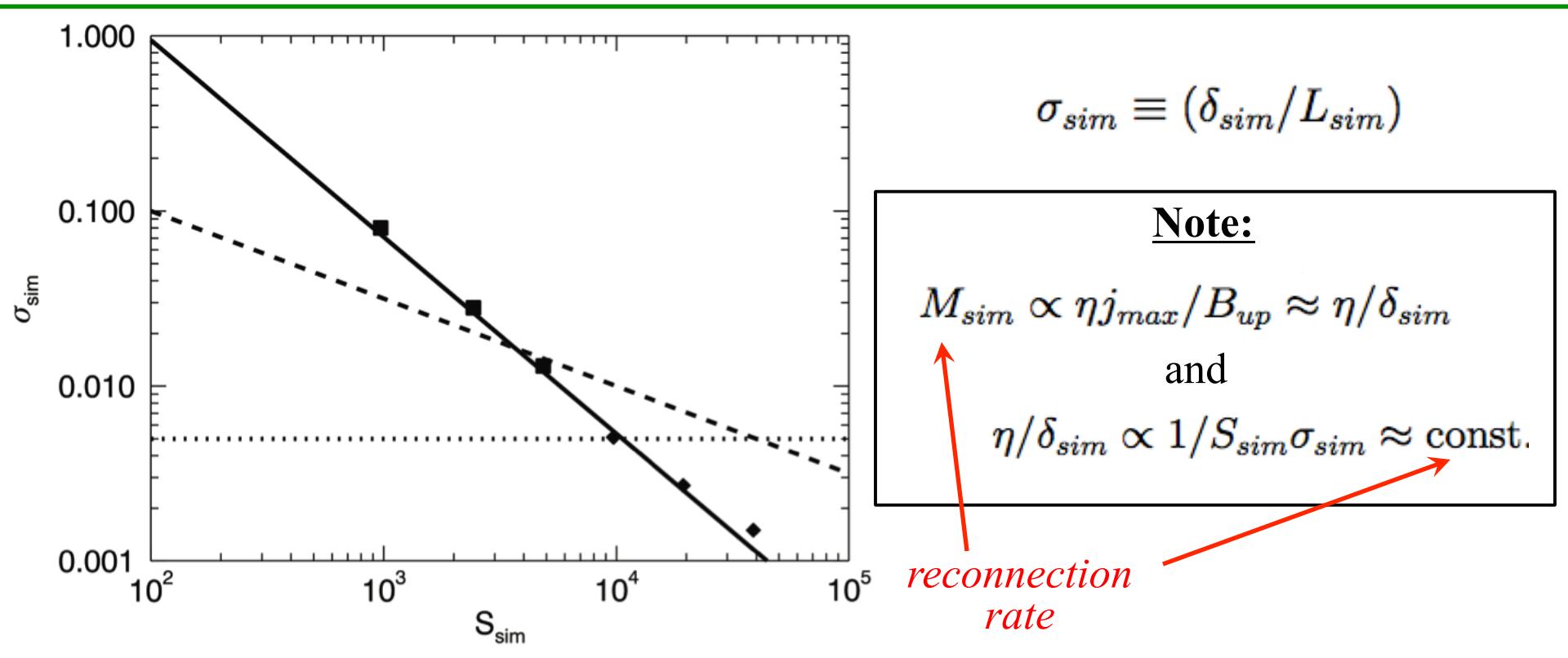
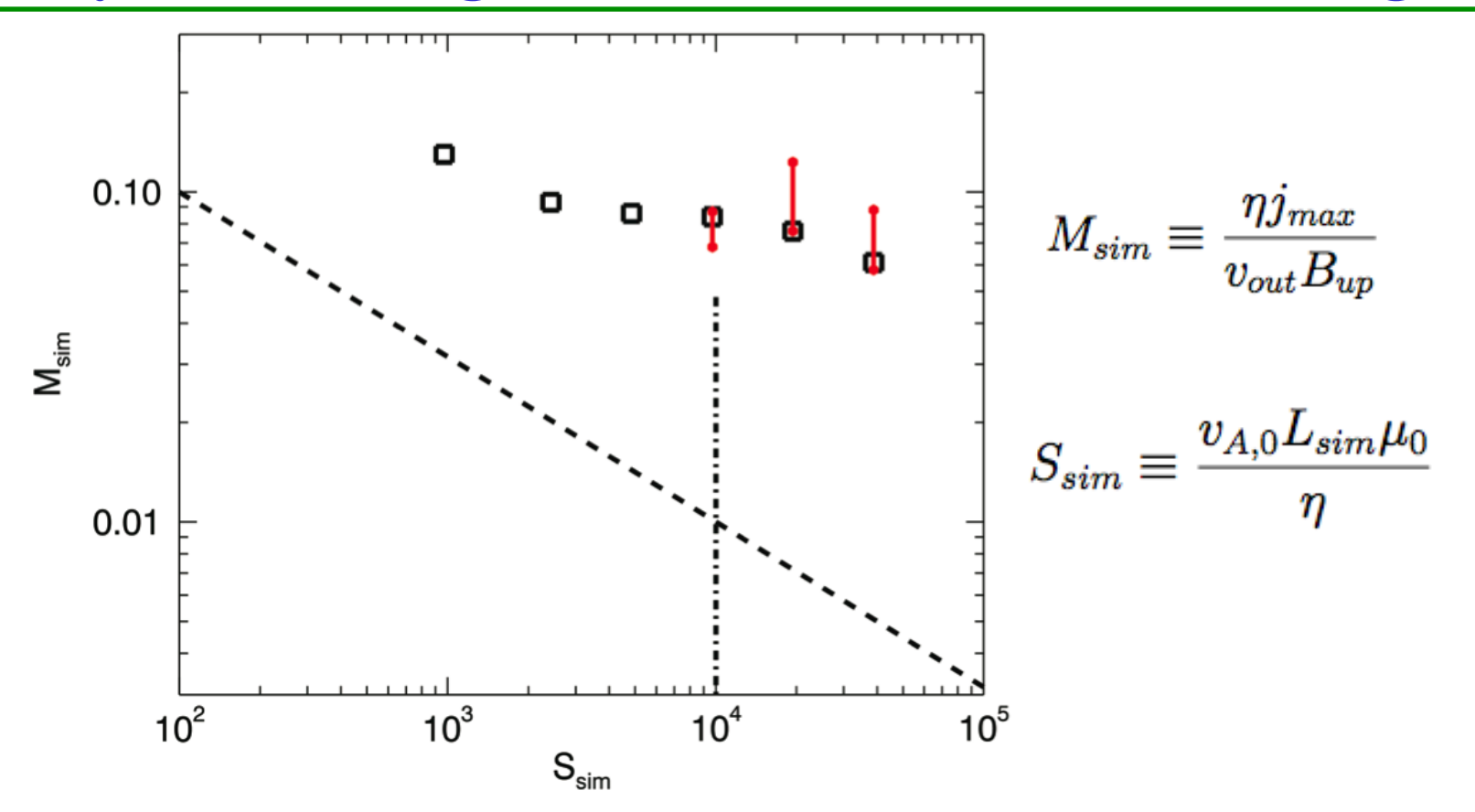


Fig. 7.— Scaling of simulation current sheet aspect ratio σ_{sim} with Lundquist number (S_{sim}) . The squares are simulations where no secondary (plasmoid) instability is seen, and the diamonds are simulations where plasmoids are observed. The dotted line is the theoretical aspect ratio at which the plasmoid instability sets in. The dashed line is the Sweet-Parker scaling law ($\propto \sqrt{1/S}$). The solid line shows a line of best fit of the data to a power law. The exponent in the power law is -1.1 ± 0.17 . This solid line intersects the $\sigma_{sim} = 1/200$ line at approximately $S_{sim} = 10^4$.



Weakly Ionized Regime: Reconnection Rate Scaling

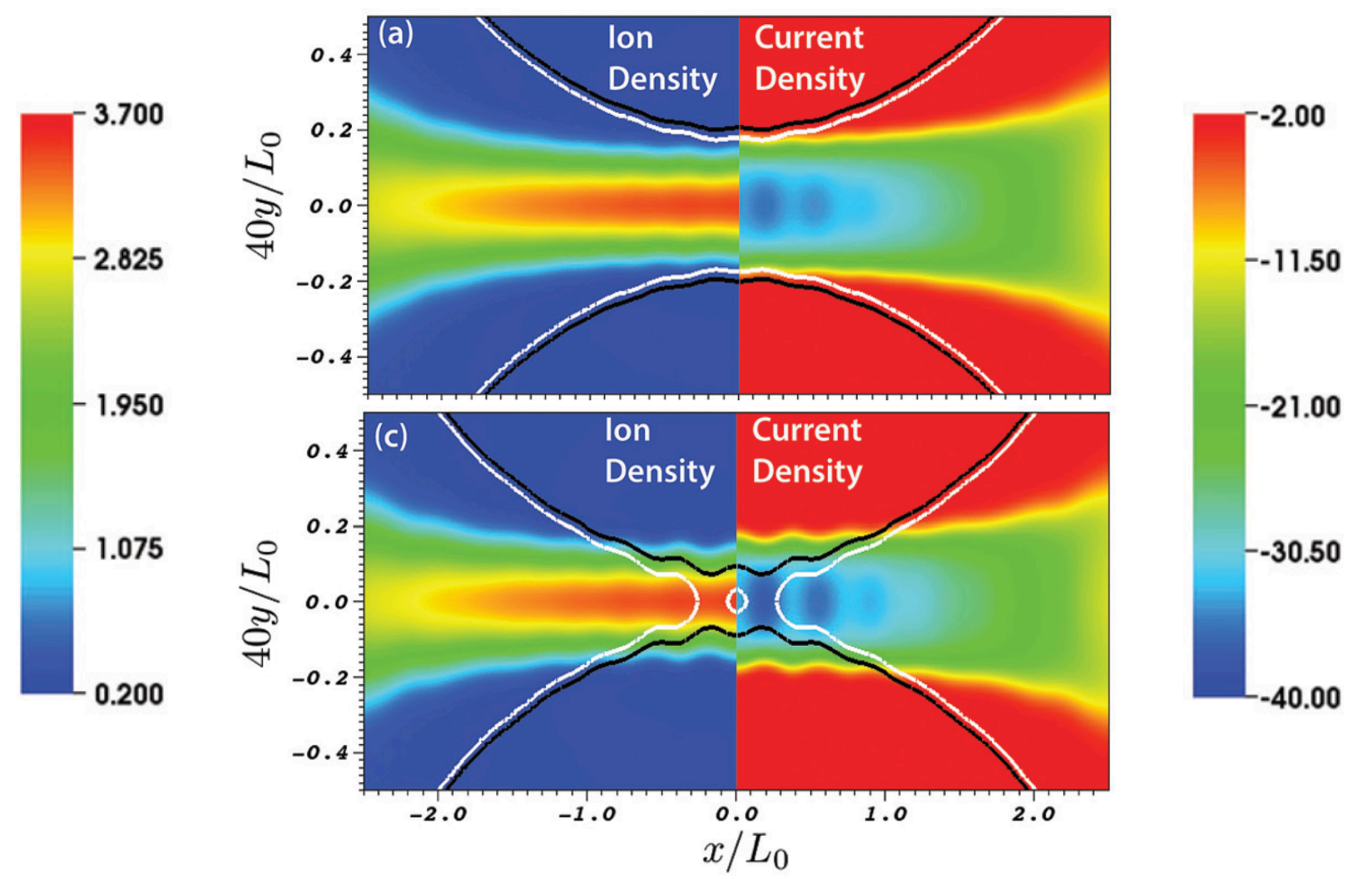


Normalized magnetic reconnection rate M_{sim} as a function of the Lundquist number. The red lines show the range in reconnection rate taken in three plasmoid-unstable simulations, after the plasmoids are formed.

The dashed line is the Sweet–Parker scaling law M \propto S^{-1/2}.



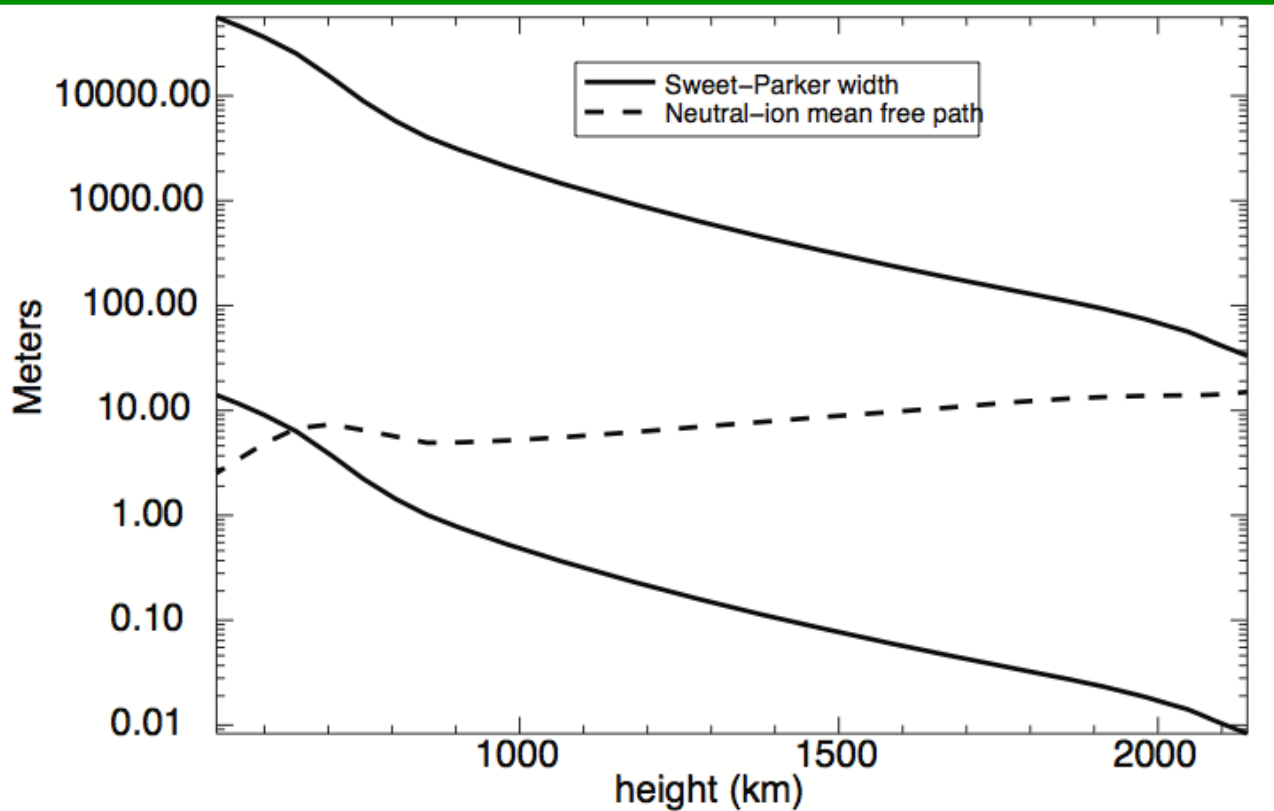
Weakly Ionized Regime: Plasmoid Instability



Highly elongated reconnection current sheets generate plasmoid structures with an order of magnitude electron density enhancement over the background electron density.



Chromosphere: Current Sheet width vs. λ_{ni}



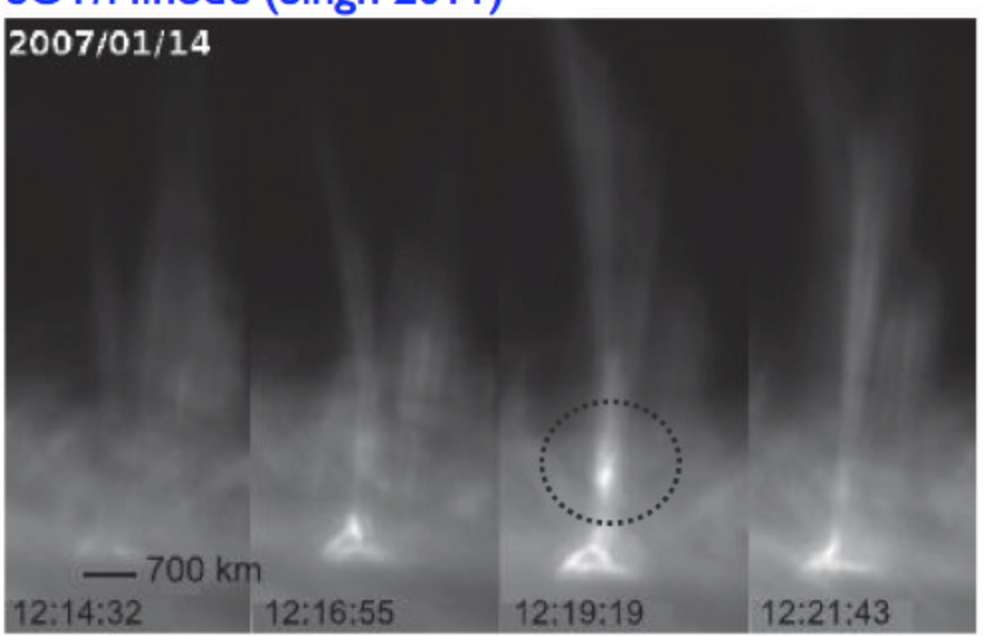
Calculation with the FALC 1D solar chromosphere model.

- Solid lines show two extremes of the calculations of the resistive width. The higher value uses a current sheet aspect ratio $\sigma = 1/1000$ and B=5 G, and the lower uses $\sigma = 1/50$ and B=1000 G.
- \triangleright The dot-dashed line is the neutral-ion collisional mean free path, λ_{ni} .
- Conclusion: Chromosphere is likely to have recombination-dominated magnetic reconnection sites with "clumps" of higher electron density



Asymmetric Chromospheric Reconnection

Chromospheric anenome jet observed with SOT/Hinode (Singh 2011)



Shibata et al. (2007)

corona
transition region
chromosphere

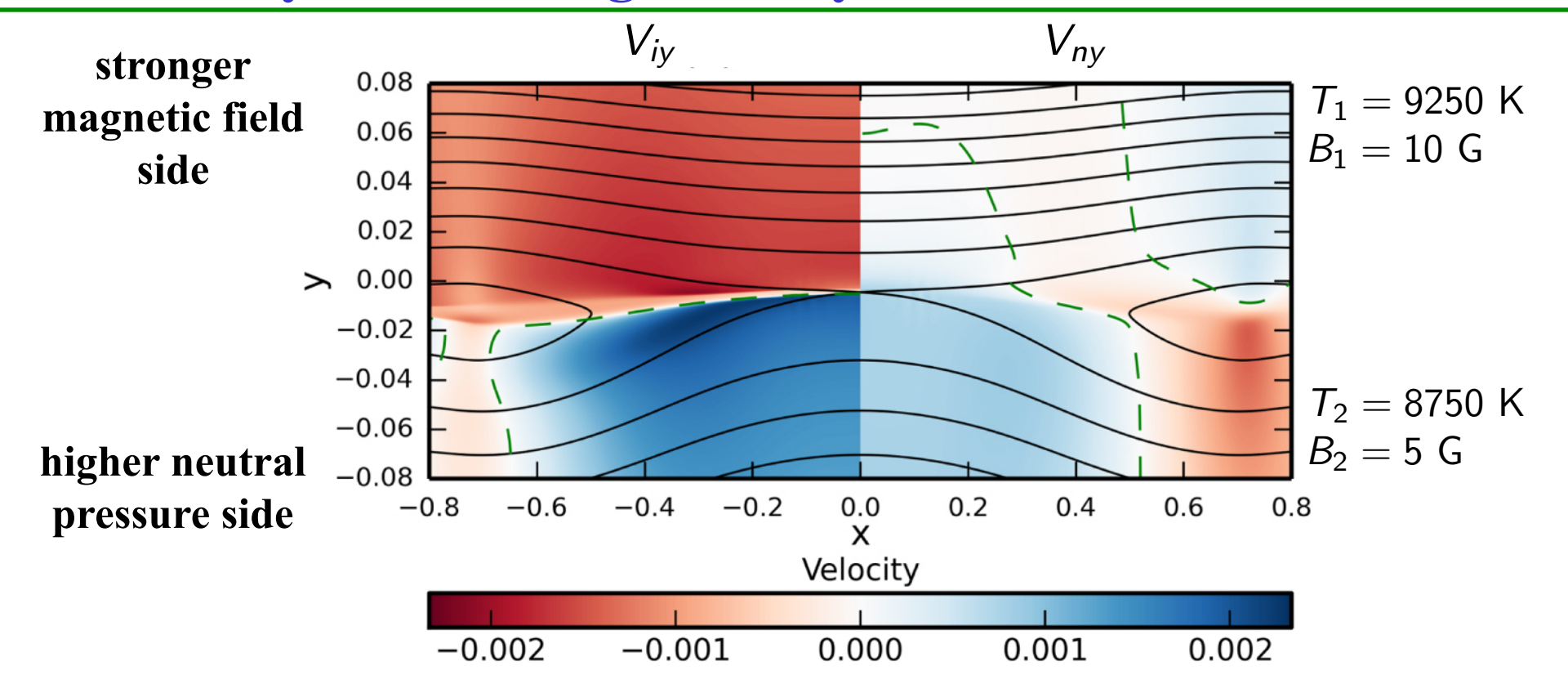
photosphere

10²km

Chromospheric jets occur when newly emerged flux reconnects with preexisting overlying flux – asymmetric reconnection



Weakly Ionized Regime: Asymmetric Reconnection

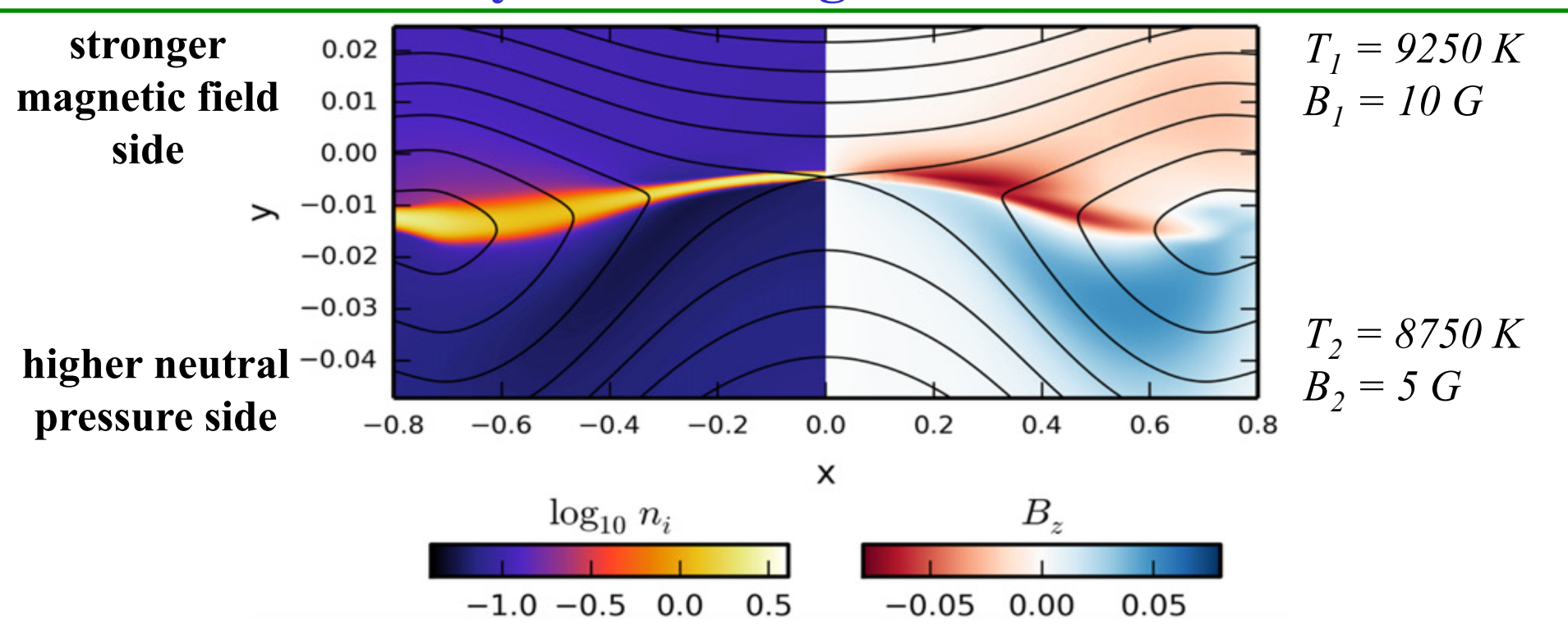


- Asymmetric decoupling between ions and neutrals in inflow
- lacktriangle Higher neutral pressure on bottom ightarrow neutrals flow upward across the current sheet

Murphy & Lukin, ApJ (2015)



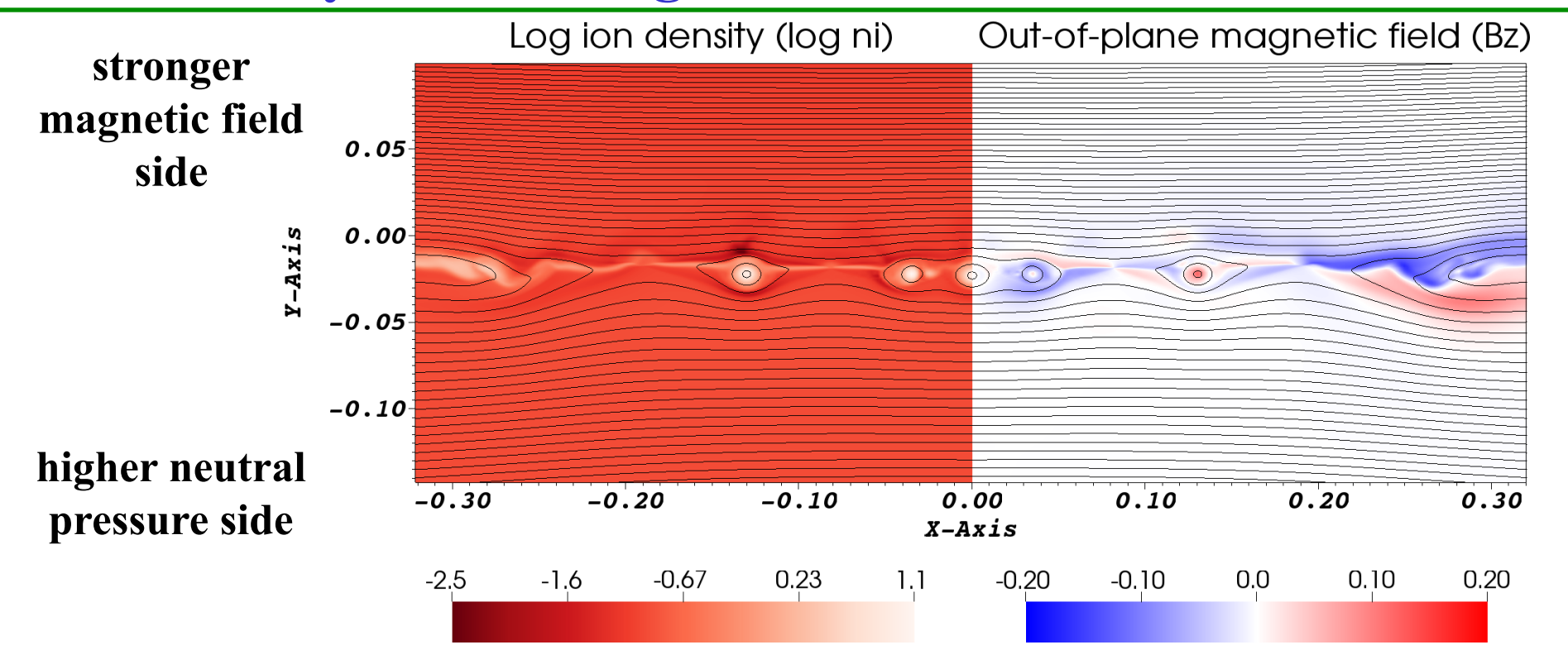
Weakly Ionized Regime: Hall effect



- > Ion-neutral coupling increases the effective ion inertial scale $(c/\omega_{pi})_{eff} = c/\omega_{pi} \times \sqrt{[(n_i + n_n)/n_i]}$
- Current sheet thinning below $(c/\omega_{pi})_{eff}$ leads to generation of out-of-plane B_z with magnitude up to 50% of reconnecting B_x component
- \triangleright Contrary to the hypothesis of Malyshkin & Zweibel, ApJ (2011), current sheet length remains macroscopic even for $\delta_{CS} < (c/\omega_{pi})_{eff}$



Weakly Ionized Regime: Plasmoids + Hall effect



- ▶ Plasmoids bulge into weak field upstream region
- High ion density in plasmoids
- Hall fields locally a large fraction of reconnecting field
 - ▶ Plasmoid instability leads to structures on $\sim c/\omega_{pi}$ scales

Slide courtesy of Nick Murphy

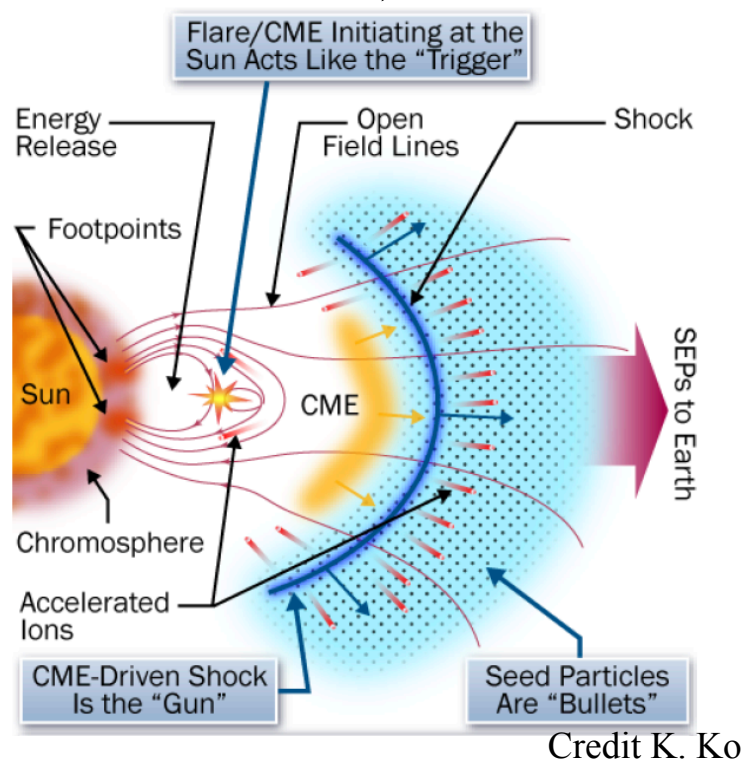


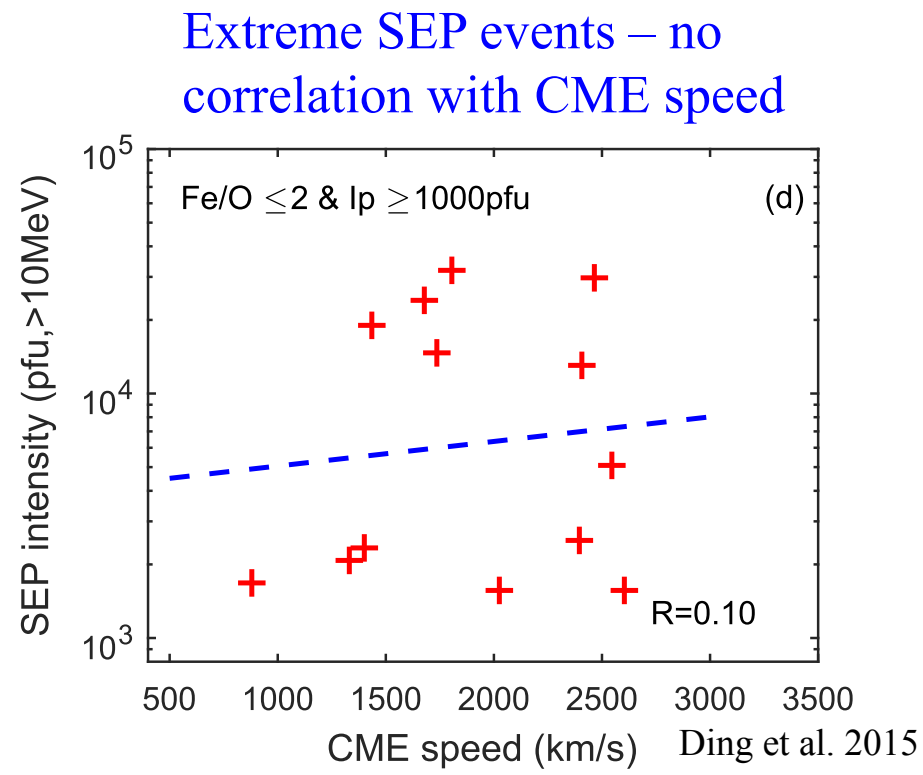
Magnetic Reconnection in a Highly Compressible Plasma of Solar Corona



SEP Production and Variability

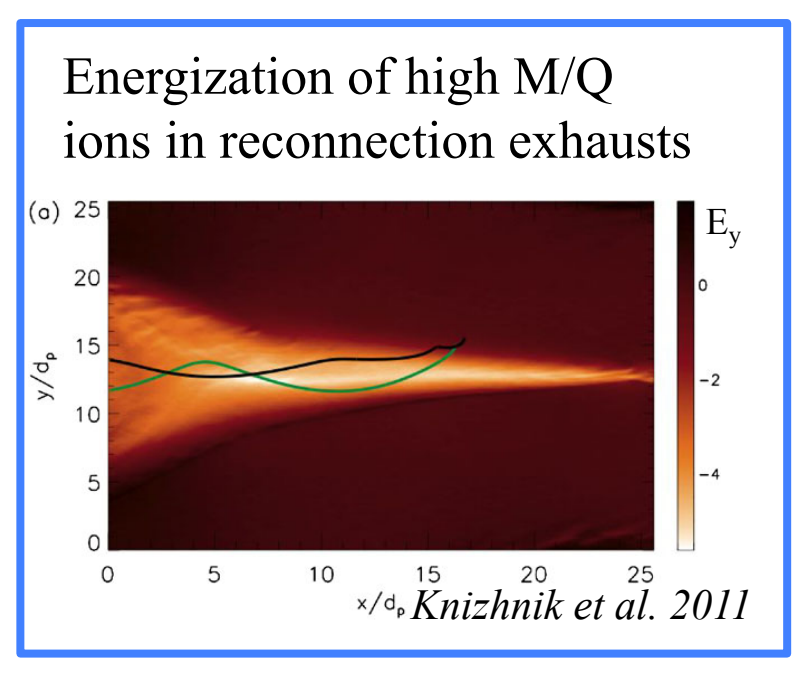
- For a given CME speed, Solar Energetic Particle (SEP) intensities vary by 3-4 orders of magnitude (Reames 2000)
- ➤ Hard spectrum of suprathermal seed particles is required for the injection into the shock acceleration process at low M_A-shocks close to the Sun (Laming et al. 2012; Zank et al. 2006)

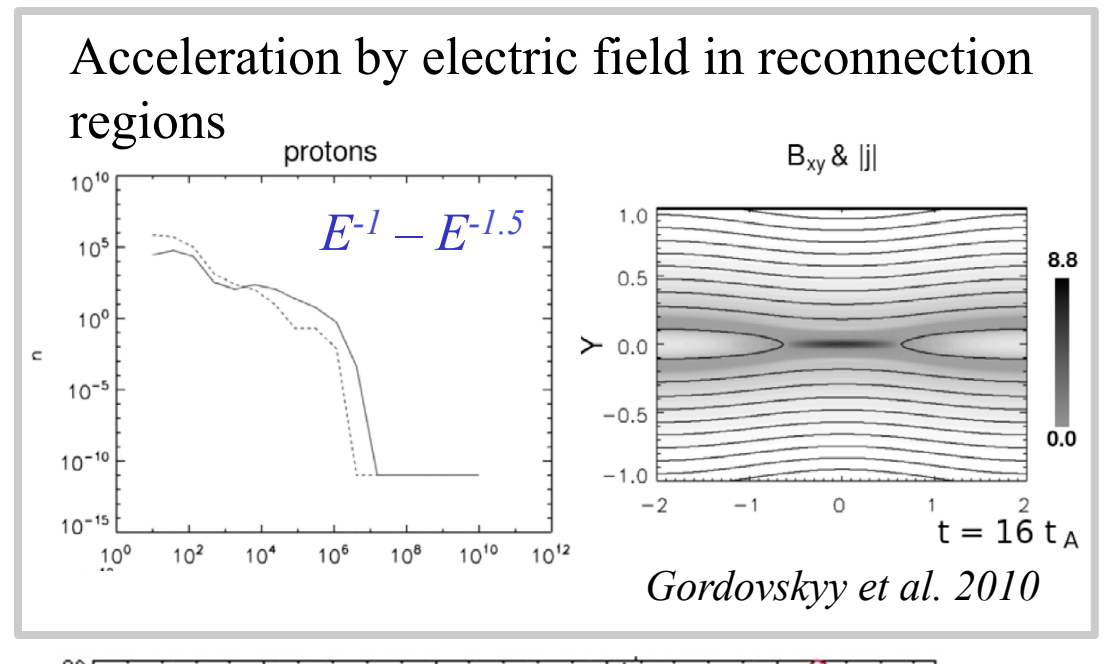






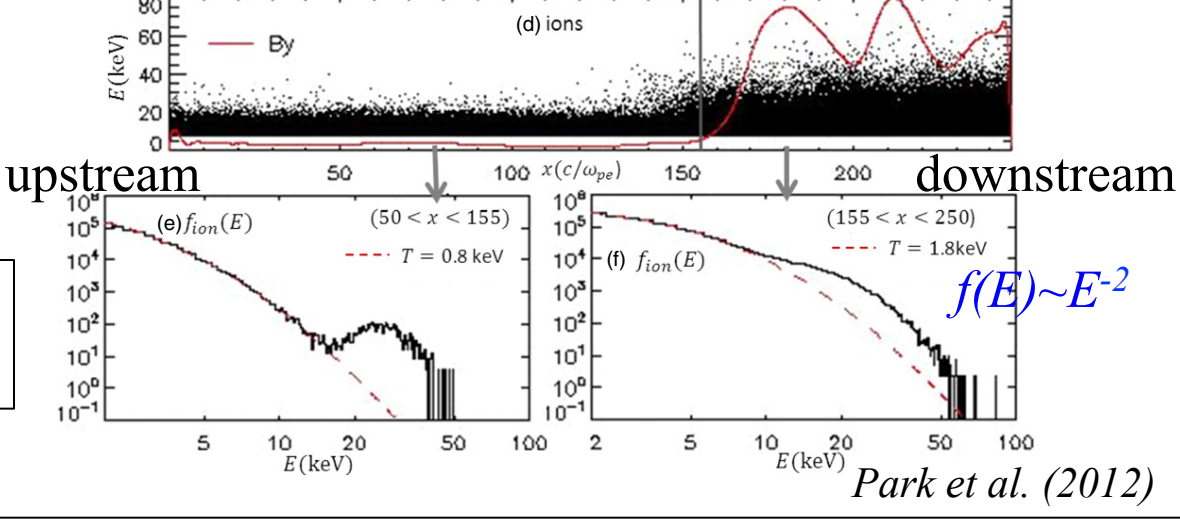
Particle Energization in Magnetic Reconnection





Drift acceleration at "termination" shocks in reconnection outflows

Acceleration can take place in multiple reconnection sites.





Particle Energization in Magnetic Reconnection

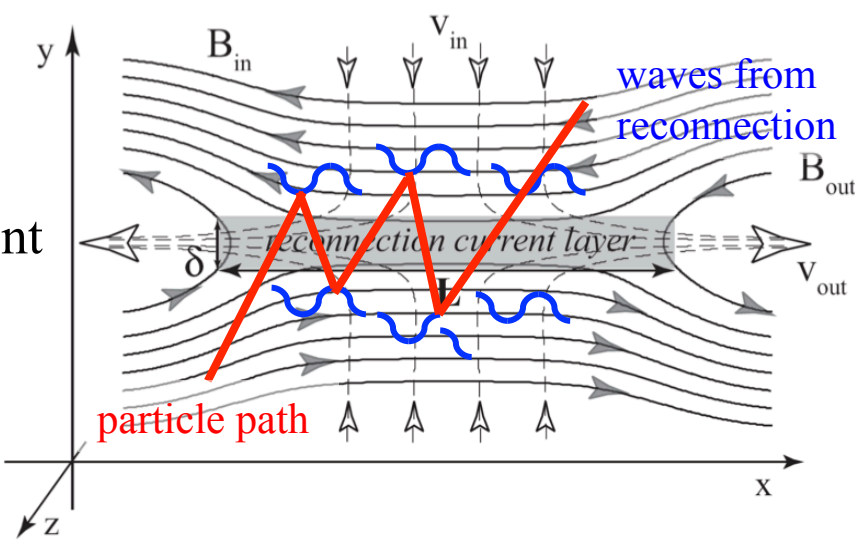
Alternative mechanism: acceleration in converging

- reconnecting flows
- > First order Fermi acceleration
- ➤ Ion's mean free path is larger than the current sheet width but smaller than its length
- > Spectrum index (Drury 2012)

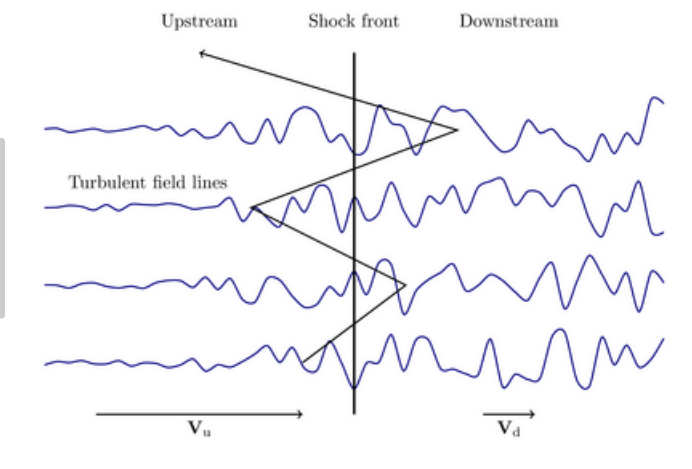
$$\frac{\partial \ln f}{\partial \ln p} = -\frac{3C}{C-1}, \quad C = \frac{n_{out}}{n_{in}}$$
 is compression

$$C >> 1$$
 $f(p) \sim p^{-3}$

How compressive can magnetic reconnection be in the solar corona?

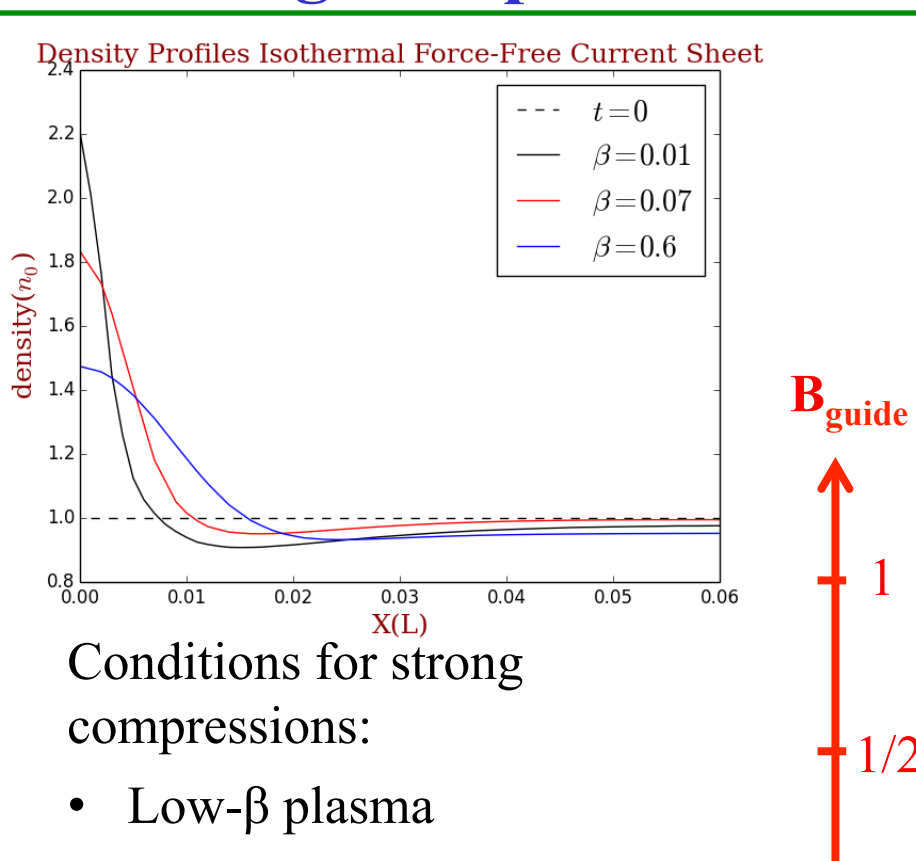


Similar to diffusive shock acceleration





Strong Compression in Reconnection Current Sheets



- Small guide field B_z
- Efficient cooling by thermal conduction and/or radiative cooling

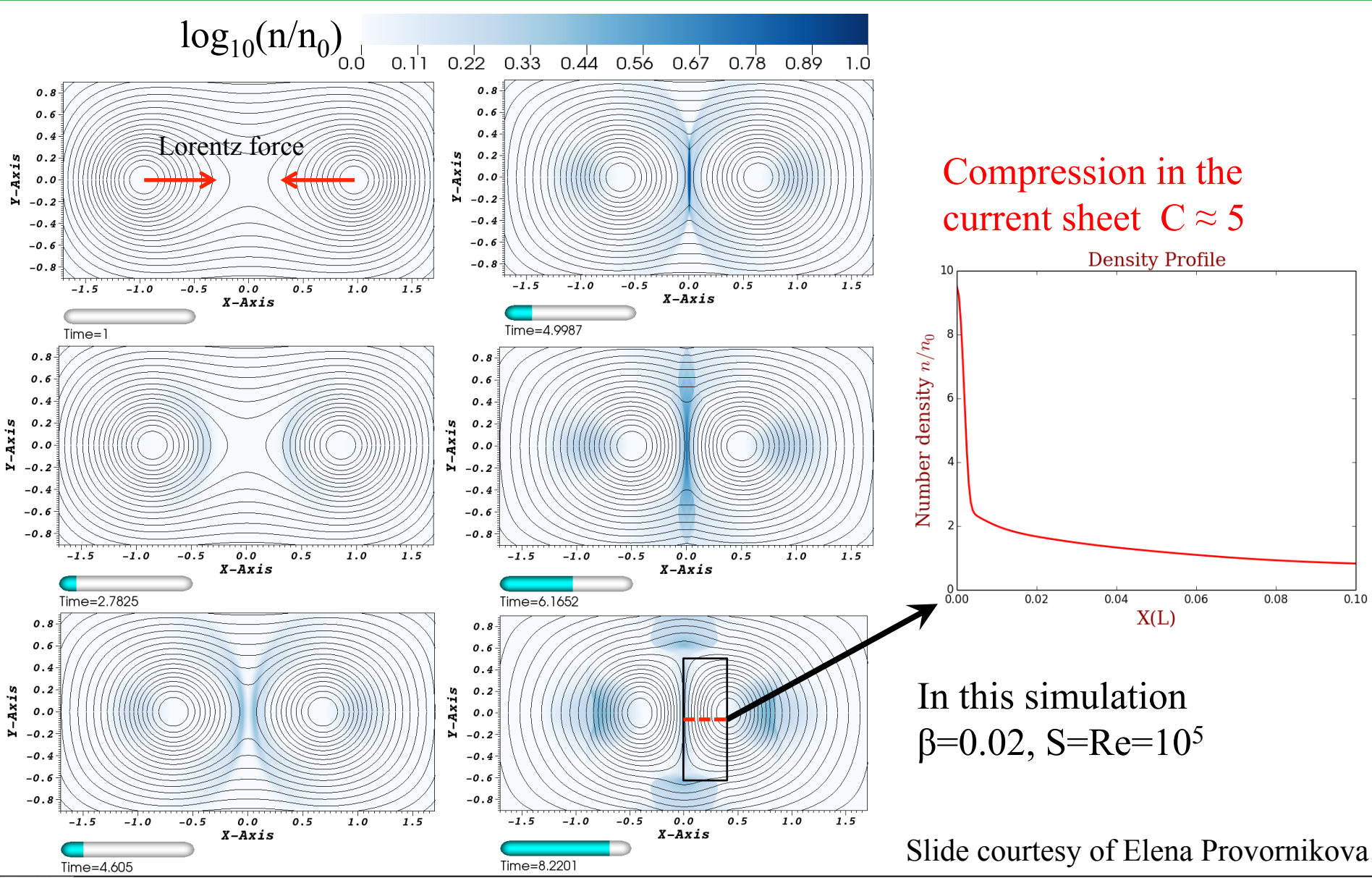
Resulting compression *C* in different configurations

7	Model Magnetic configuration	Isothermal β=0.02	Isothermal β=0.8	2T Full MHD β=0.8
	Force-free current sheet	C ≈ 3.5	C ≈ 1.4	C ≈ 1
	Reduced guide field	C ≈ 5	C ≈ 1.5	C ≈ 4
	Harris current sheet	C≈6	C ≈ 1.6	

In all simulations $S = Re = 10^4$



Merging and Reconnection of Magnetic Flux Ropes





Vyacheslav (Slava) Lukin, "Magnetic Reconnection in the Lower Solar Atmosphere" University of Michigan – Ann Arbor, September 19th, 2016

Compression in Reconnection of Magnetic Flux Ropes

Parametric study

Model Plasma beta	Isothermal MHD model	2T Full MHD model (including thermal conduction and radiative cooling)
β=0.02	C ≈ 5	C ≈ 3
β=0.07	C ≈ 3.5	C ≈ 2
β=0.6	C ≈ 1.6	C ≈ 1



Key Questions in Magnetic Reconnection

➤ How fast can the magnetic energy be released?

➤ How is it possible that under some circumstances free magnetic energy can be slowly accumulated and then explosively released?

➤ What determines the released energy partition between thermal, radiation, bulk flow and non-thermal particles?

➤ Under what circumstances the reconnection sub-volumes are localized in 1D (a current sheet), 2D (a line current) and 3D (a point-like current density concentration)?



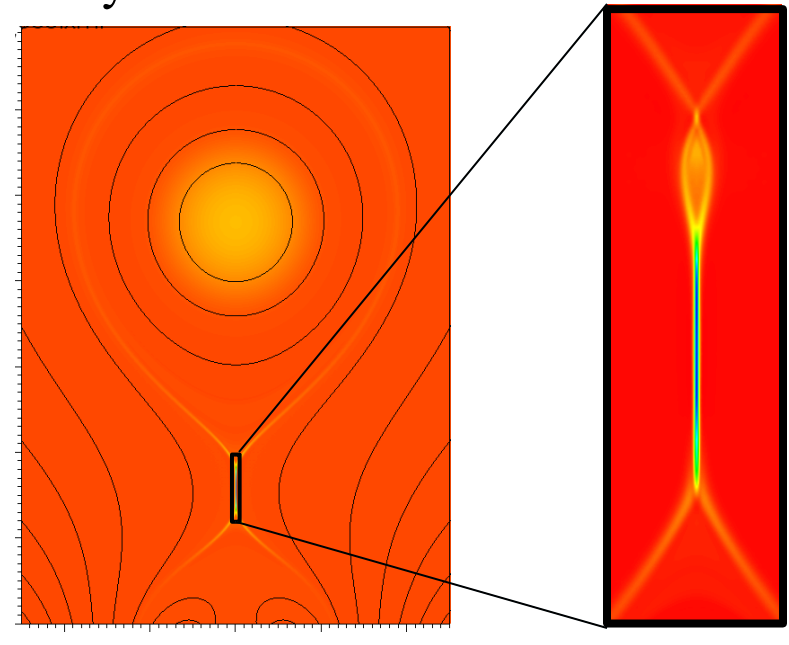
Conclusions I

- ➤ Magnetic reconnection in a weakly ionized plasma can be "fast" or "slow", depending on scale separation between the neutral-ion collisional scale and the resistive scale. In the chromosphere, both regimes are possible allowing for slow build-up of magnetic stress by photospheric forcing, followed by fast release via current sheets thinner than the neutral-ion coupling scale.
- The scale separation in the inflow and nearly perfect outflow coupling leads to rapid formation of high aspect ratio current sheets that are prone to onset of secondary instabilities and generation of "clumps" of higher electron (and ion) density within small-scale magnetic flux tubes.
- The Hall effect does not seem to impact the reconnection rate for current sheets thinner than $(c/\omega_{pi})_{eff}$ but still thicker than c/ω_{pi} .
- Asymmetry in the plasma parameters of the reconnecting magnetic structures can lead to particle transport across the current sheet
- So far, we have only explored a small part of the surface area of the spherical cow of magnetic reconnection in a weakly ionized plasma...



Conclusions II

- ➤ Magnetic reconnection sites with high plasma compressions in the lower solar atmosphere are the potential locations where suprathermal particles can be produced with hard energetic spectrum.
- Sufficient plasma compressions ≥ 4 can be achieved in reconnection regions at magnetic nulls that are omnipresent in the solar corona.
- Further, enhanced emission may be expected from magnetic nulls in the lower corona/transition region due to density enhancements.
- ➤ Ongoing and future work includes a study of plasmoid generation in low beta current sheets behind erupting flux ropes, their impact on particle energization, and diagnostic of CME-associated reconnection sites via a study of heavy ion charge states within CMEs at 1 AU.





Extra Slides



Recent Publications Reporting HiFi Simulations: 2012-16

- E.T. Meier, et al., "Modeling open boundaries in dissipative MHD simulation," JCP **231**, 2963 (2012)
- O. Ohia, et al., "Demonstration of anisotropic fluid closure capturing the kinetic structure of magnetic reconnection," PRL 109, 115004 (2012)
- J.E. Leake, et al., "Multi-fluid simulations of chromospheric magnetic reconnection in a weakly ionized reacting plasma," ApJ 760, 109 (2012)
- A. Le, et al., "Regimes of the electron diffusion region in magnetic reconnection," PRL 110, 135004 (2013)
- J.E. Leake, et al., "Magnetic reconnection in a weakly ionized plasma," PoP 20, 061202 (2013)
- A. Stanier, et al., "Two-fluid simulations of driven reconnection in the Mega-Ampere Spherical Tokamak," PoP 20, 122302 (2013)
- D.A. Schaffner, et al., "Turbulence analysis of an experimental flux rope plasma," PPCF **56**, 064003 (2014)
- P. K. Browning, et al., "Self-organization during spherical torus formation due to flux rope merging in the Mega-Ampere Spherical Tokamak," PPCF **56**, 064009 (2014)
- S.D. Knecht, et al., "Effects of a conducting wall on Z-pinch stability," IEEE Transactions on Plasma Science 42, 1531 (2014)
- D.A. Schaffner, et al., "Temporal and spatial turbulent spectra of MHD plasma and an observation of variance anisotropy," ApJ 790, 126 (2014)
- E. Lee, et al., "On flux rope stability and atmospheric stratification in models of coronal mass ejections triggered by flux emergence," A&A 569, A94 (2014)
- J.E. Leake, et al., "Ionized plasma and neutral gas coupling in the Sun's Chromosphere and Earth's Ionosphere/Thermosphere," SSRv **184**, 107-172 (2014)
- N.A. Murphy & V.S. Lukin, "Asymmetric magnetic reconnection in weakly ionized chromospheric plasmas," ApJ 805, 134 (2015)
- O. Ohia, et al., "Scaling laws for magnetic reconnection, set by regulation of the electron pressure anisotropy to the firehose threshold," GRL 42, 067117 (2015)
- P. K. Browning, et al., "Two-fluid and magnetohydrodynamic modeling of magnetic reconnection in the MAST spherical tokamak and the solar corona," PPCF **58**, 014041 (2016)
- C. Akcay, et al., "A Two-Fluid Study of Oblique Tearing Modes in a Force-Free Current Sheet," PoP 23, 012112 (2016)
- E. Provornikova, et al., "Plasma compressions in magnetic reconnection regions in the solar corona," ApJ **825**, 55 (2016)

